

Supporting Information

Synthesis and melt-spinning of partly bio-based thermoplastic poly(cycloacetal-urethane)s toward sustainable textiles

Niklas Warlin,^a Erik Nilsson,^{b,c} Zengwei Guo,^c Smita V. Mankar,^a Nitin Valsange,^a Nicola Rehnberg,^{a,d} Stefan Lundmark,^c Patric Jannasch^{*a} and Baozhong Zhang^{*a}

^a Centre of Analysis and Synthesis, Department of Chemistry, Lund University, P.O. Box 124, SE-22100 Lund, Sweden.

^b Plasman, Molndalsvagen 36, 412 63 Gothenburg, Sweden

^c Department of Chemistry, Biomaterials and Textile, RISE - Research Institutes of Sweden, Mölndal SE-43153, Sweden.

^d Strategic R&D, Bona AB, Box 210 74, 200 21 Malmö, Sweden.

^e Perstorp AB, Innovation, Perstorp Industrial Park, 284 80 Perstorp, Sweden.

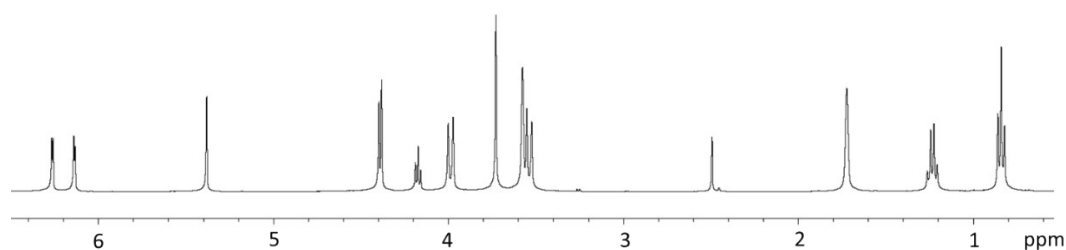


Figure S1. ¹H NMR spectrum of Monomer T.

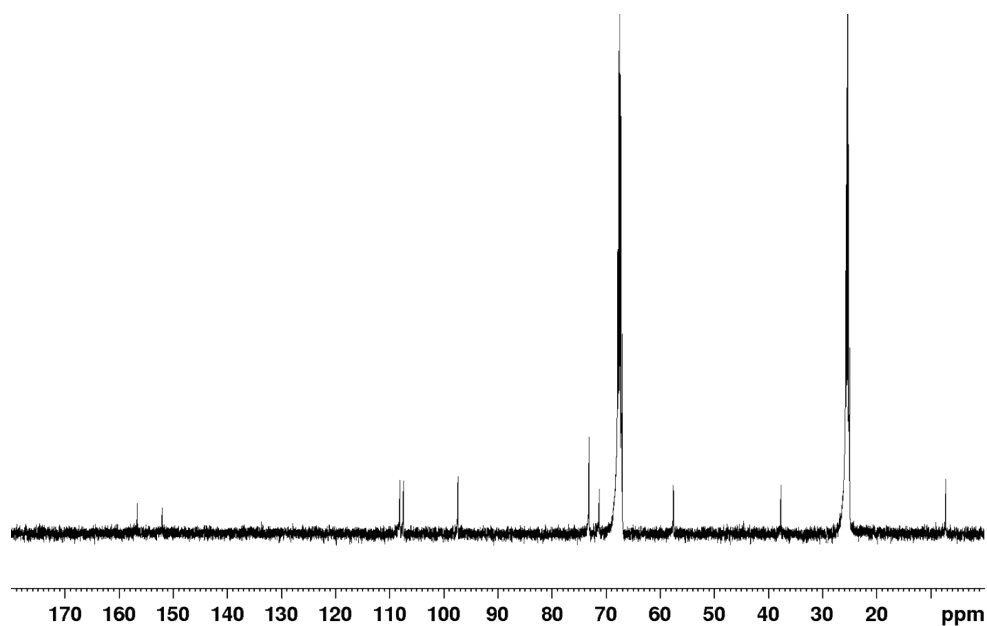


Figure S2. ¹³C NMR spectrum of Monomer T.

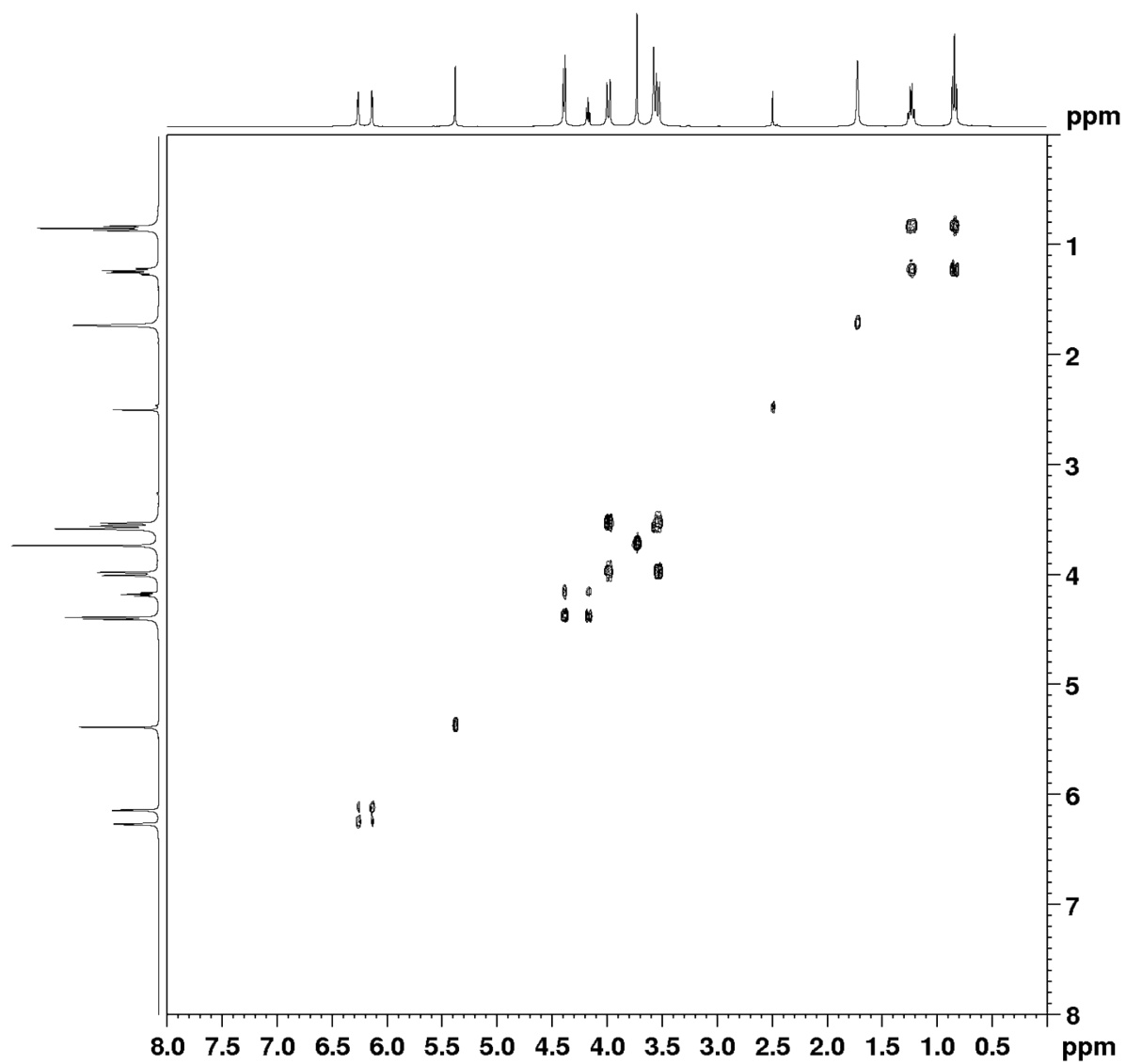


Figure S3. COSY spectrum of Monomer T.

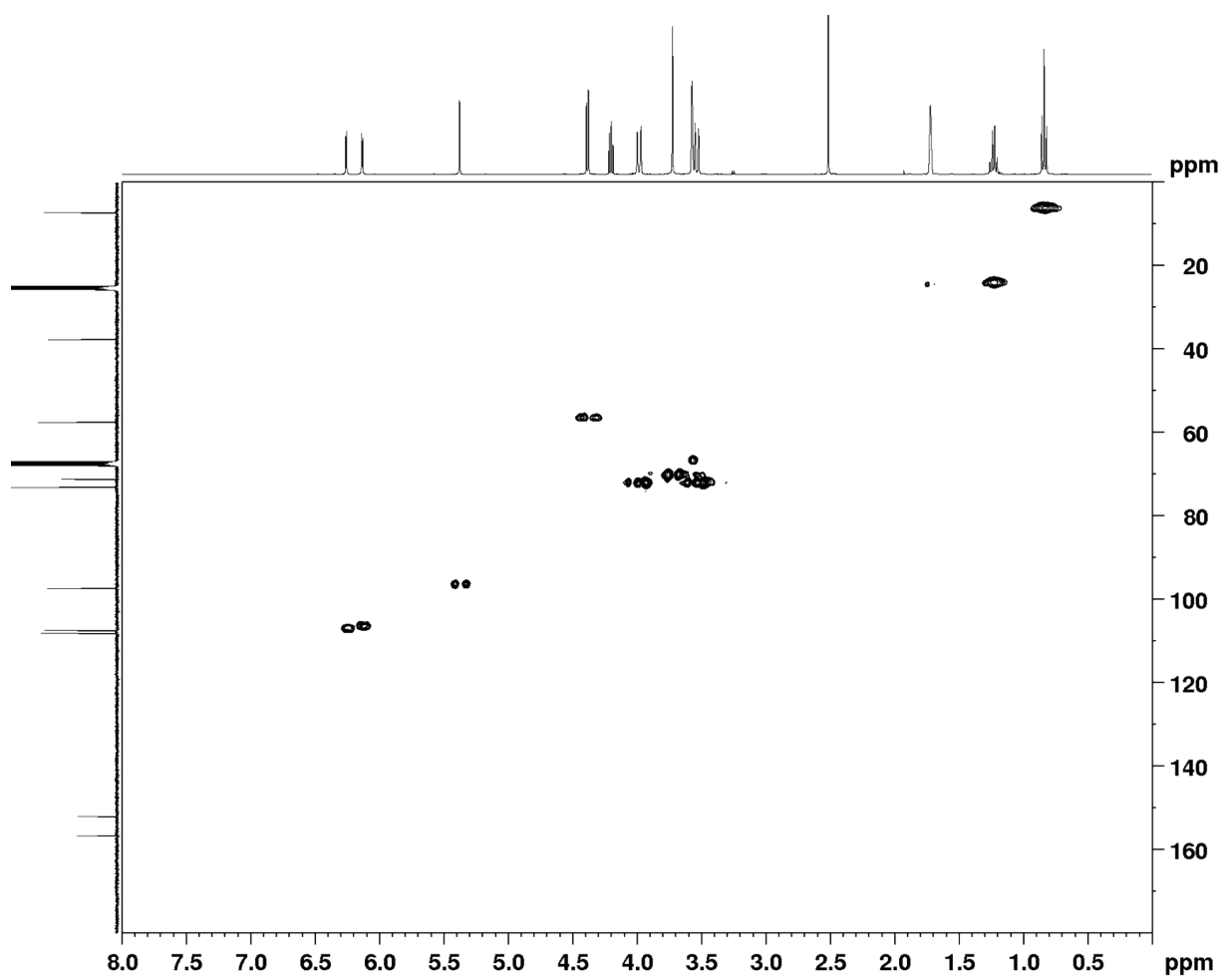


Figure S4. HMQC spectrum of Monomer T.

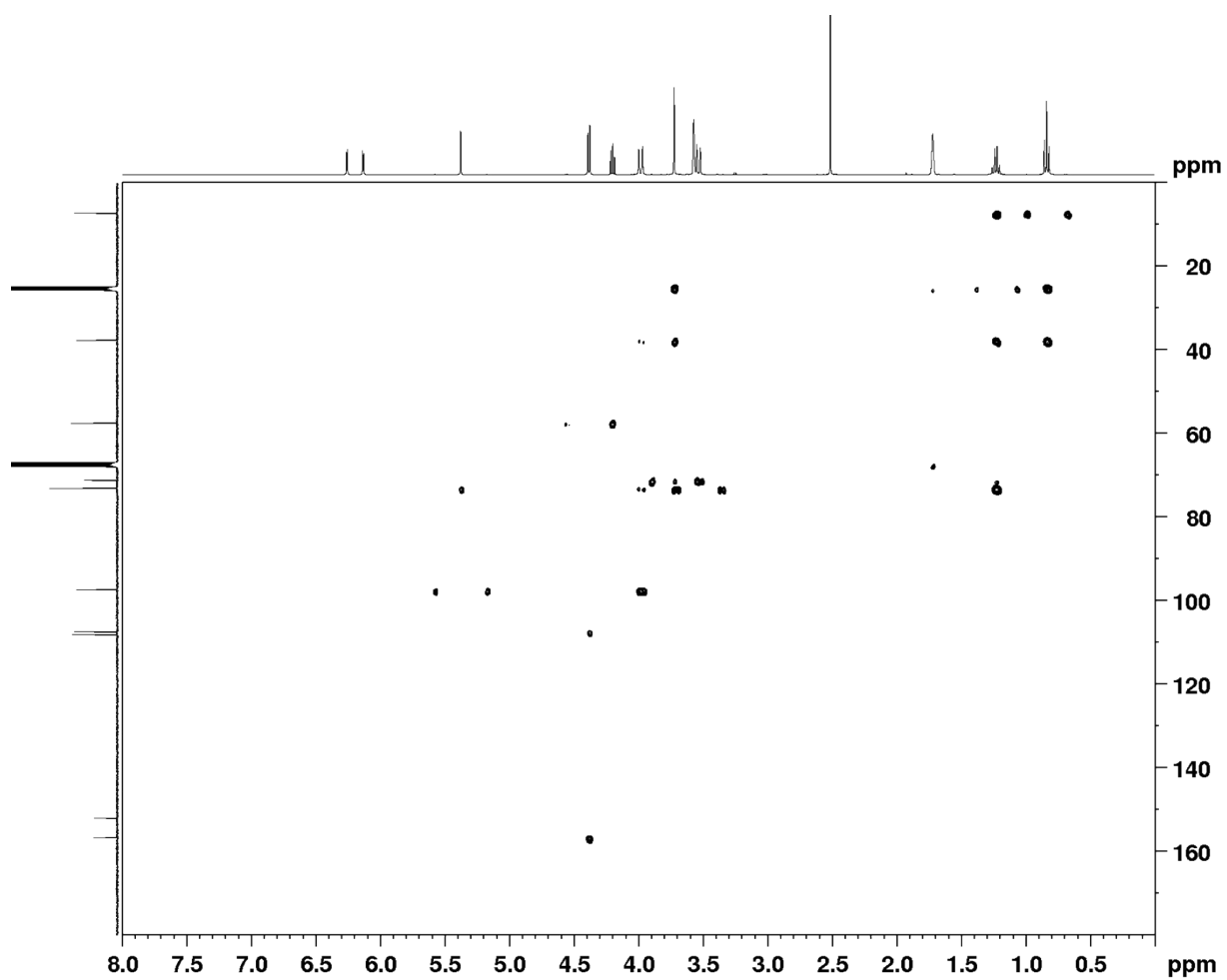


Figure S5. HMBC spectrum of Monomer T.

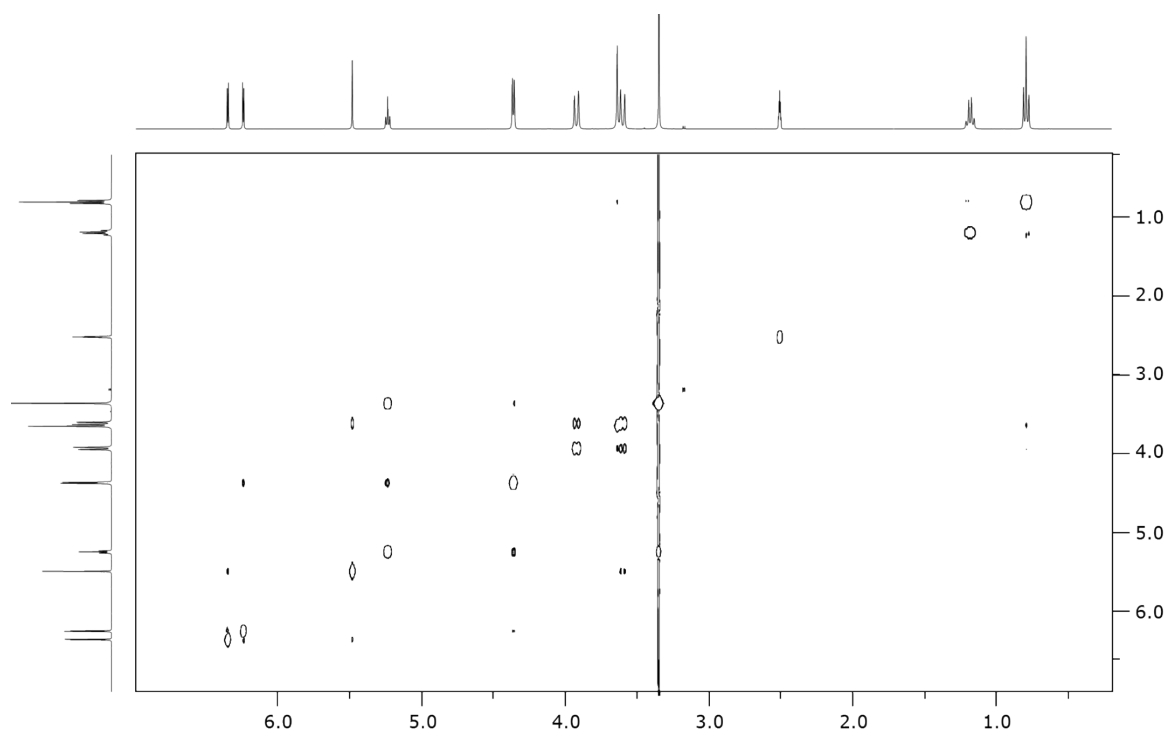


Figure S6. NOESY spectrum of Monomer T.

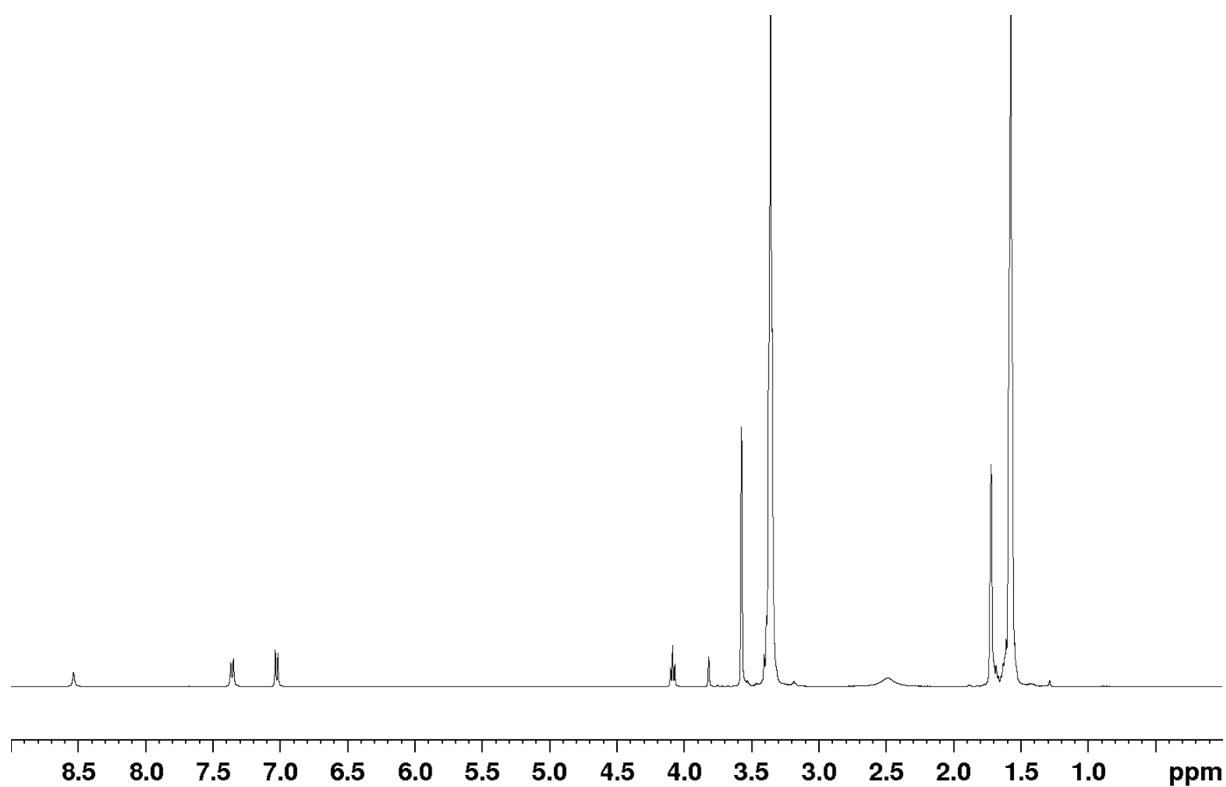


Figure S7. ^1H NMR spectrum of PAU-0.

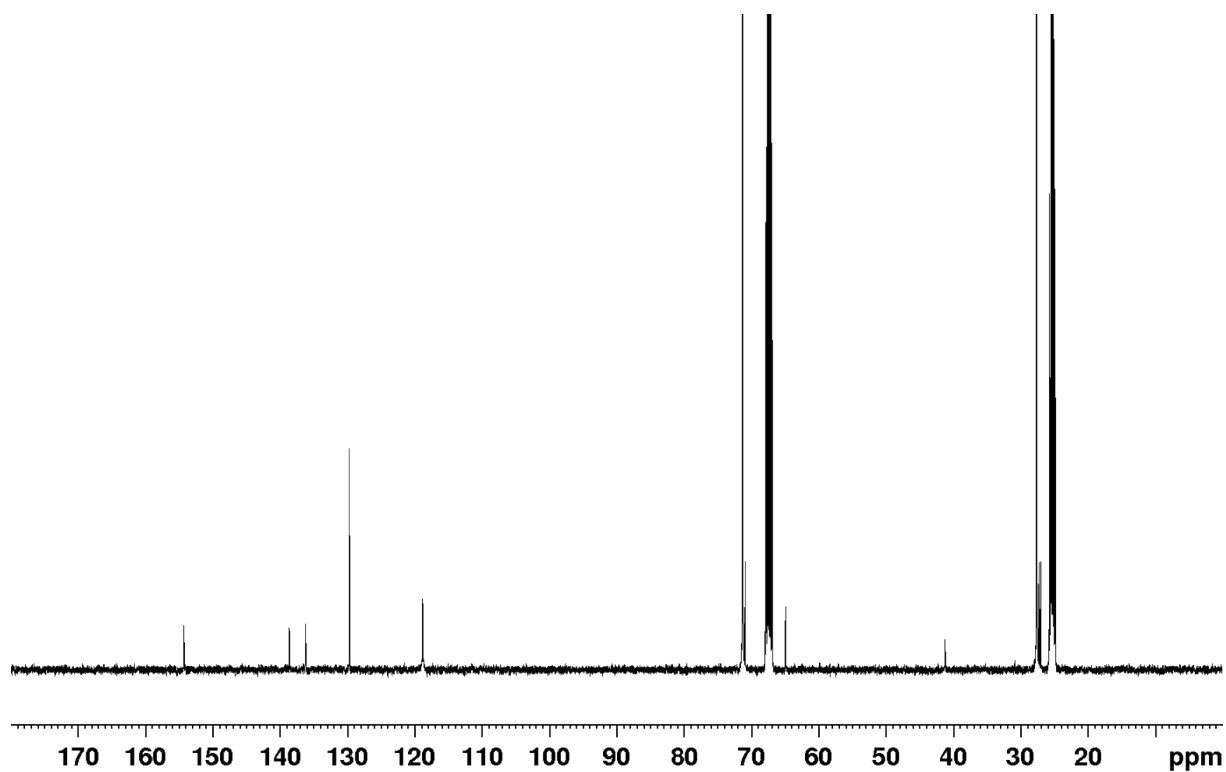


Figure S8. ^{13}C NMR spectrum of PAU-0.

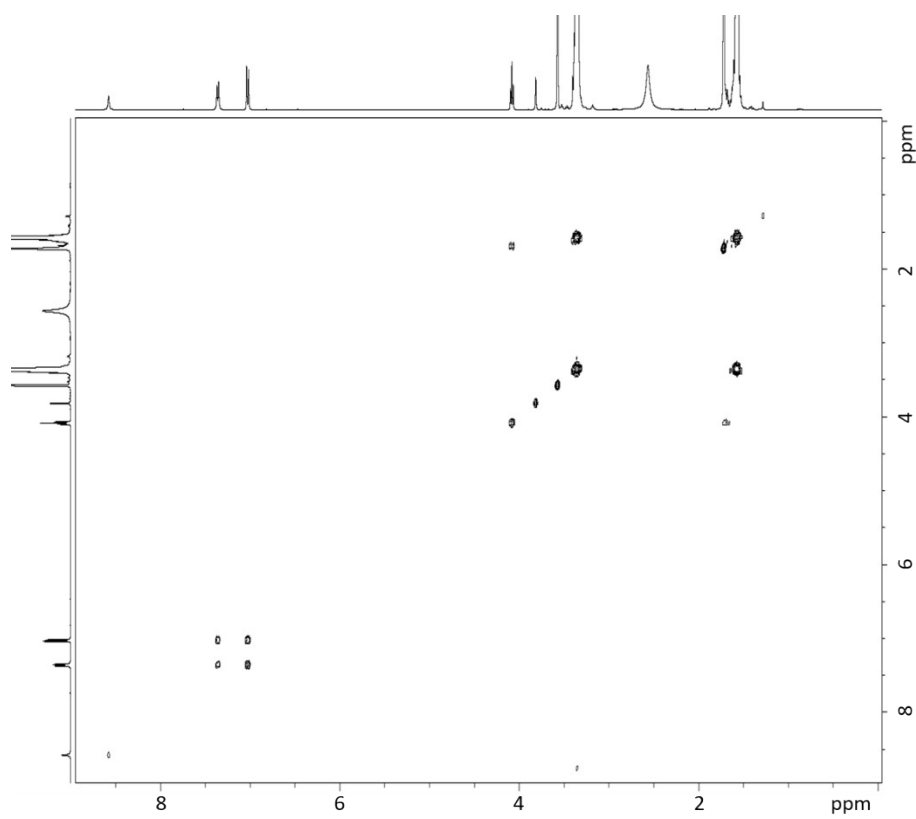


Figure S9. COSY spectrum of PAU-0.

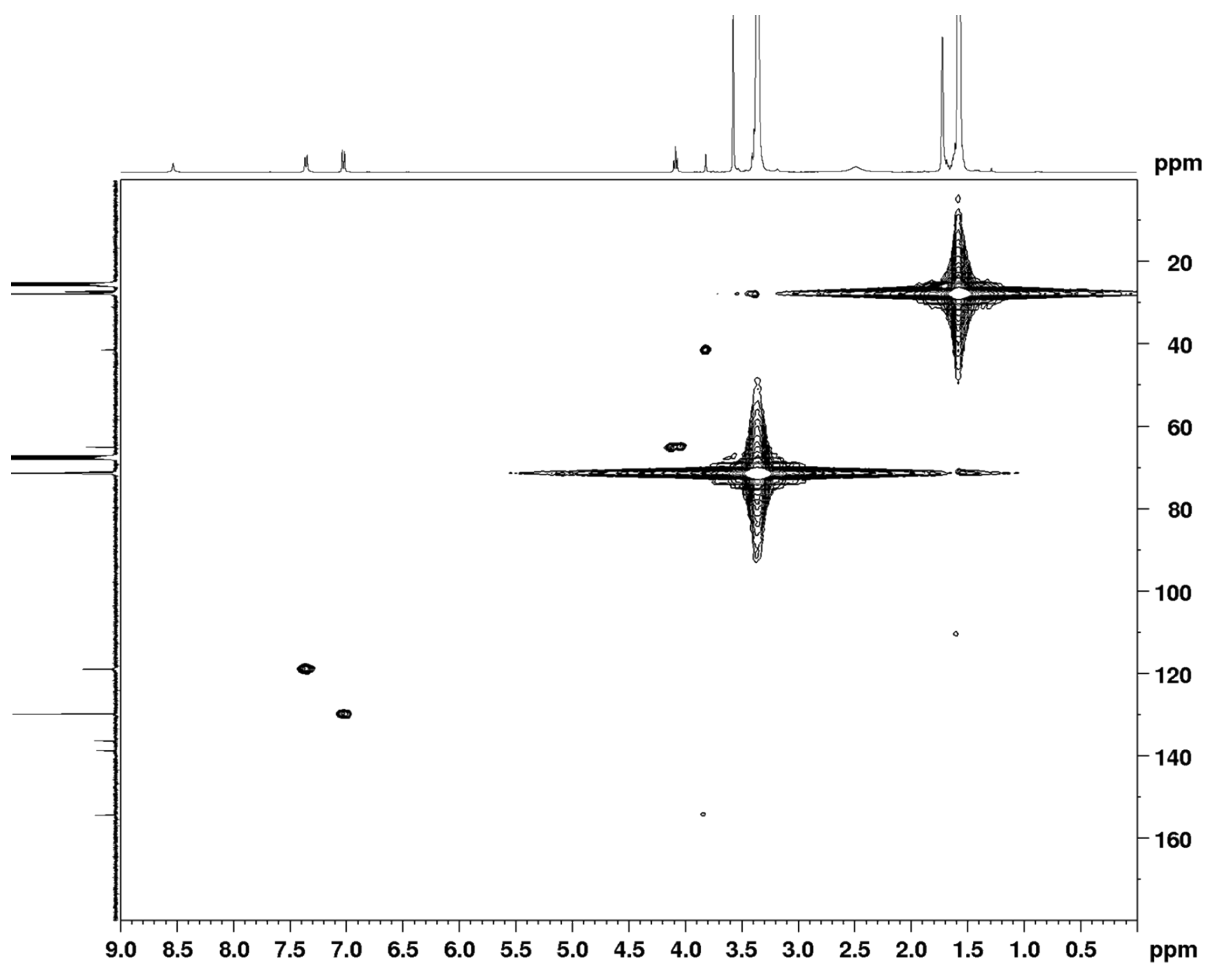


Figure S10. HMQC spectrum of PAU-0.

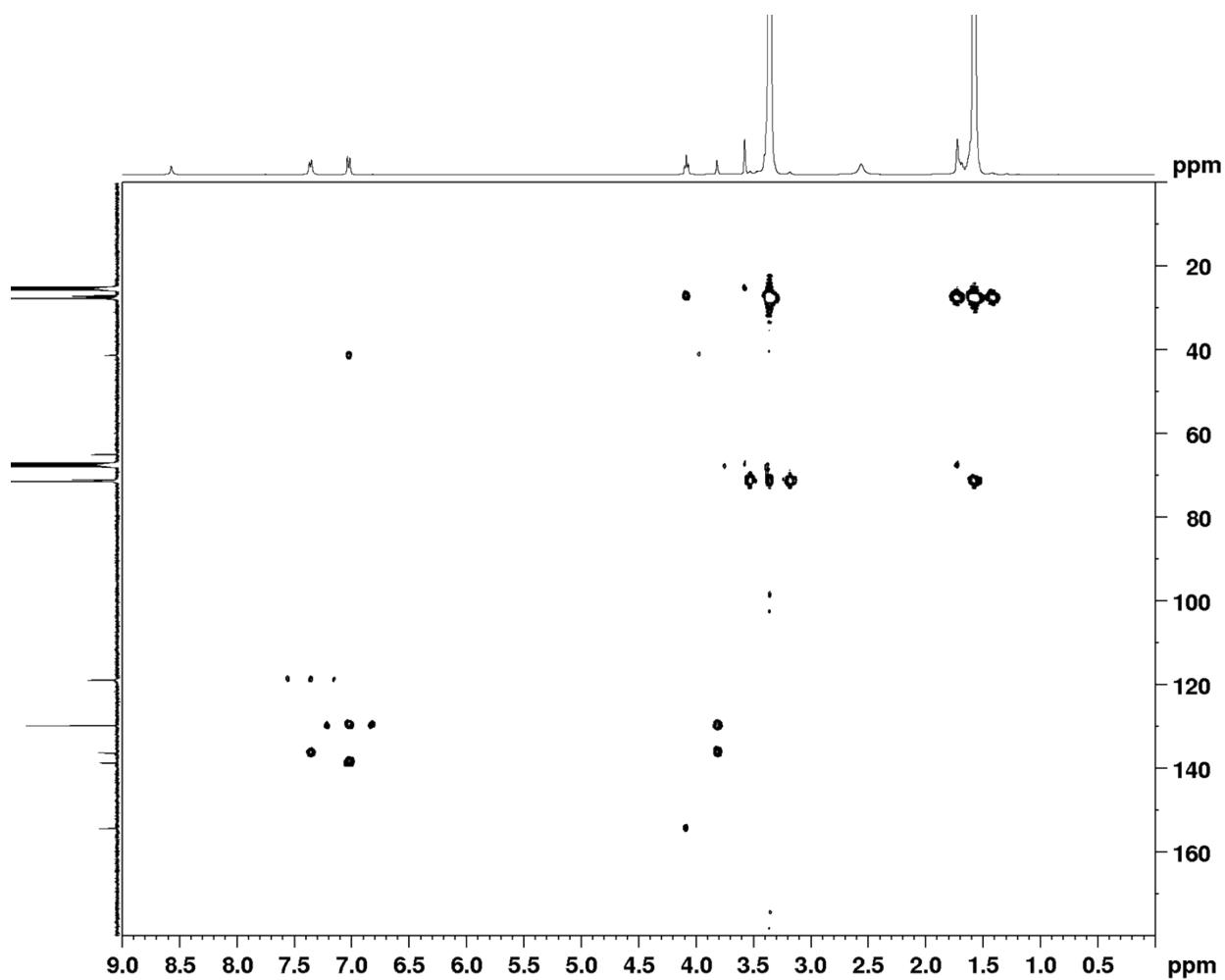


Figure S11. HMBC spectrum of PAU-0.

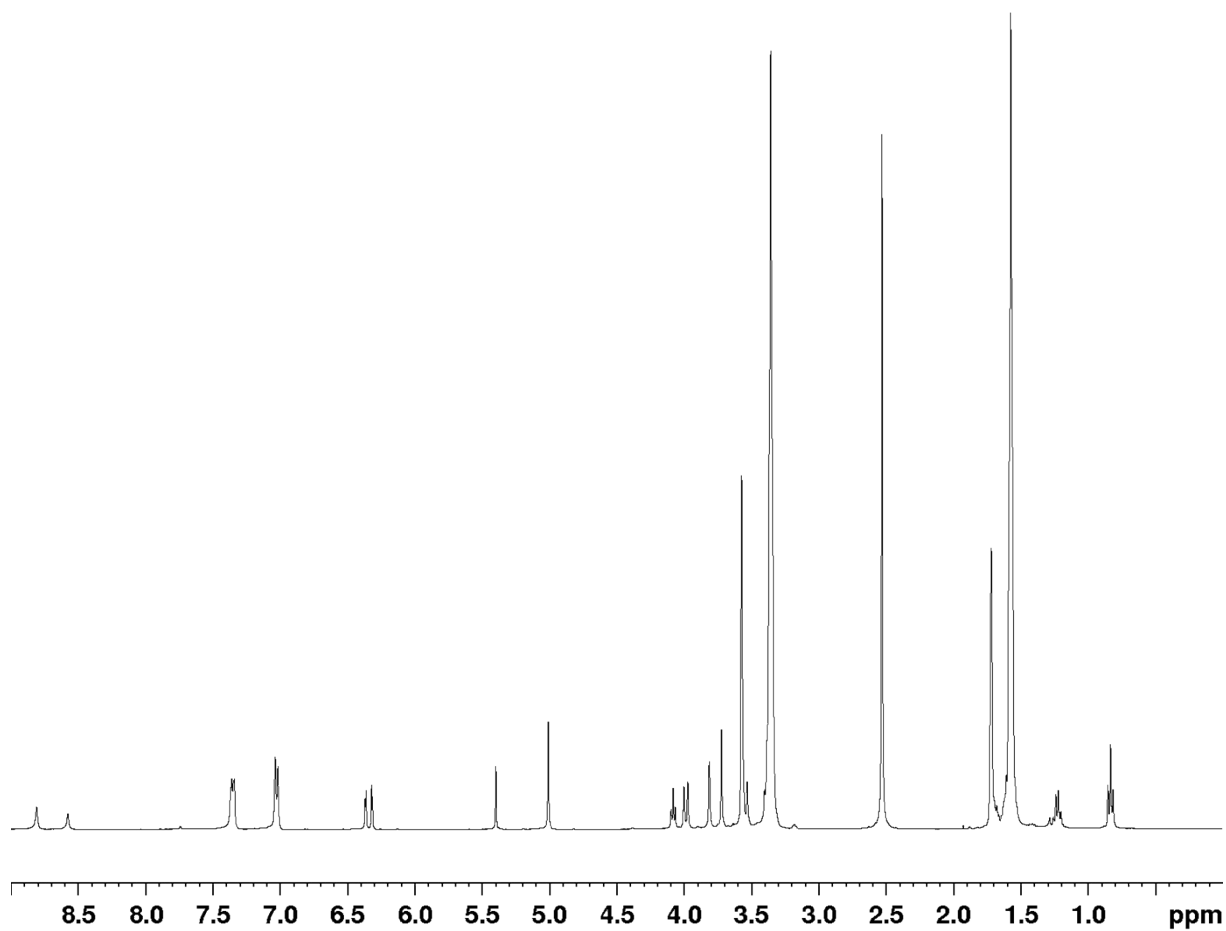


Figure S12. ^1H NMR spectrum of PAU-25.

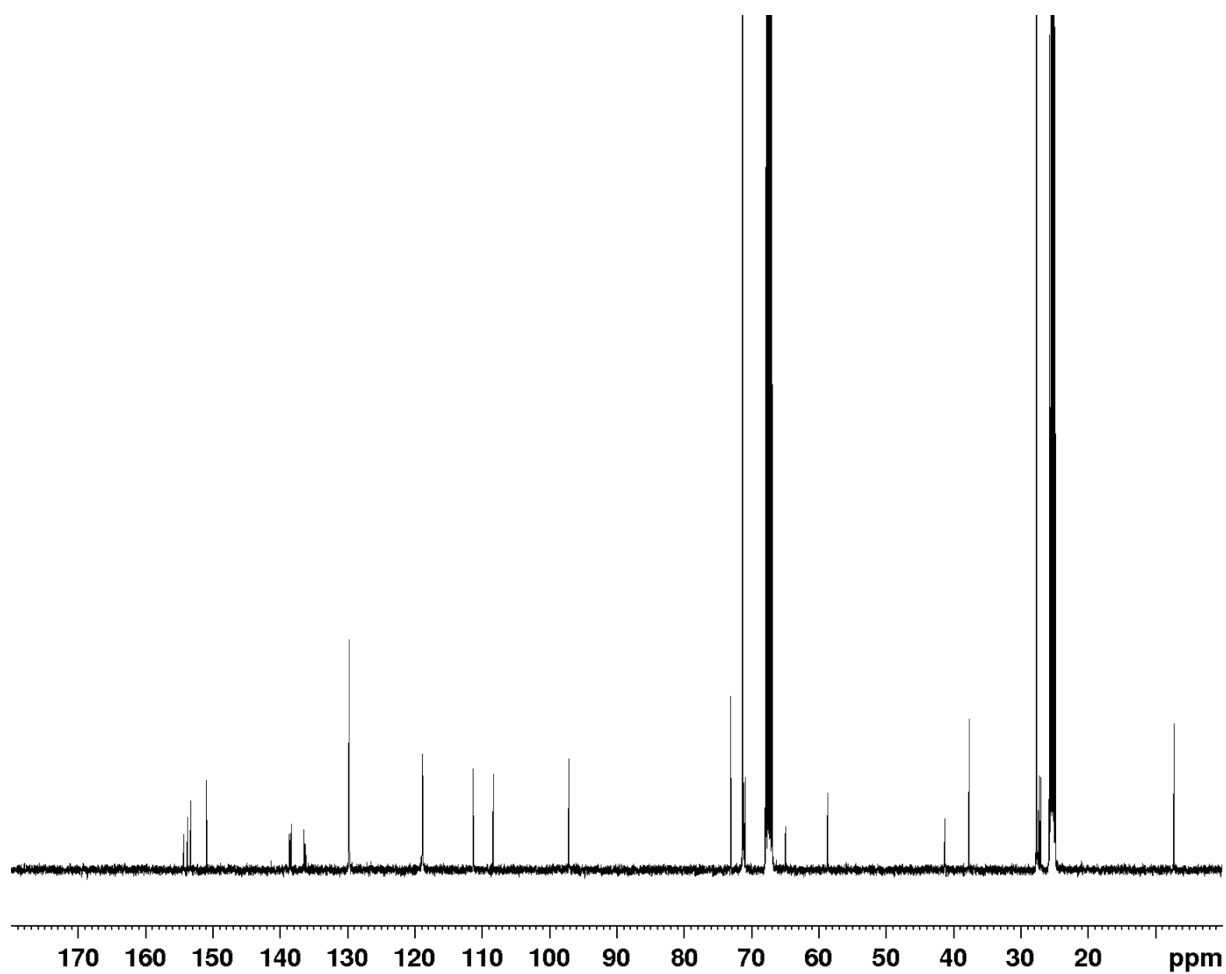


Figure S13. ^{13}C NMR spectrum of PAU-25.

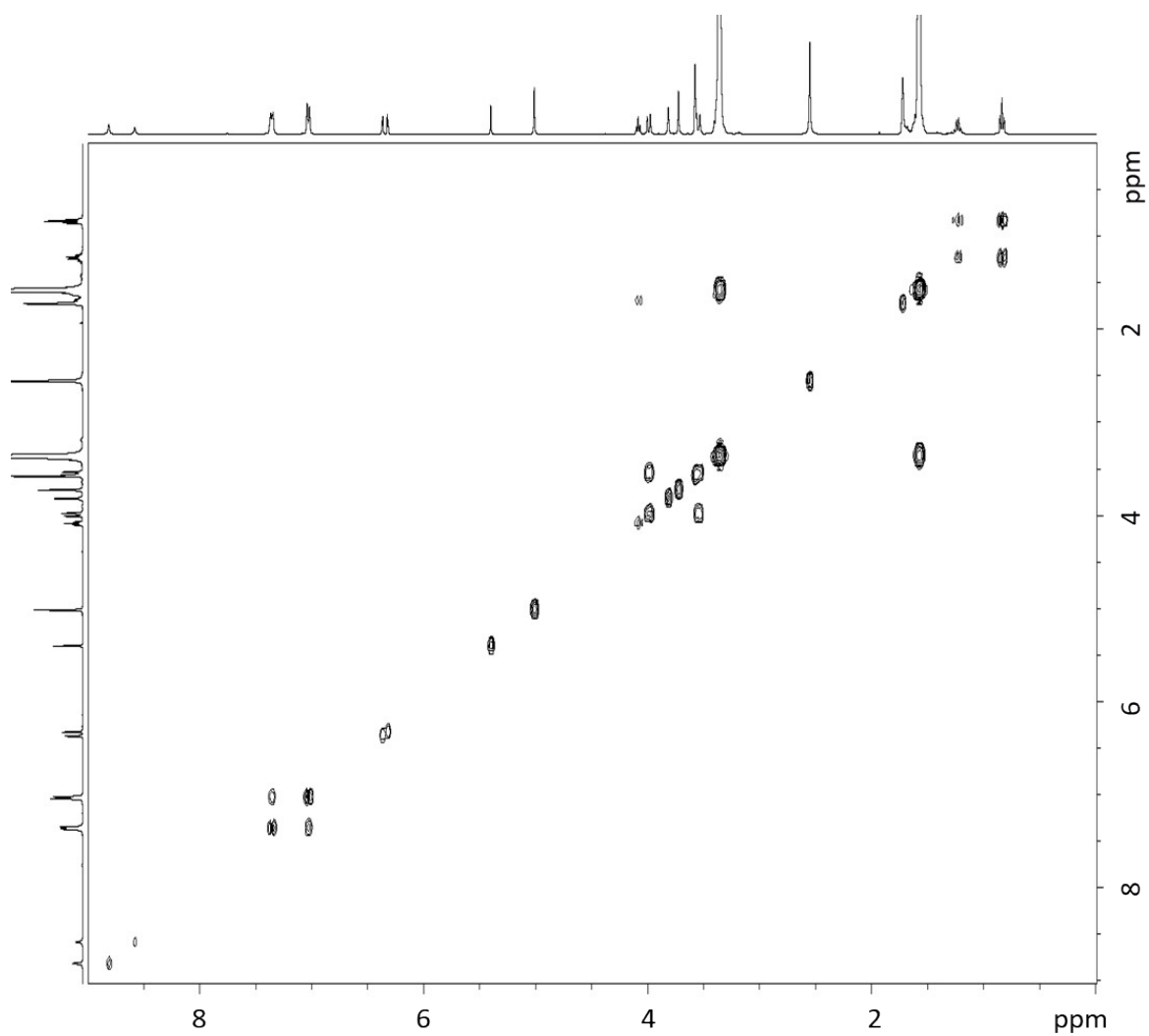


Figure S14. COSY spectrum of PAU-25.

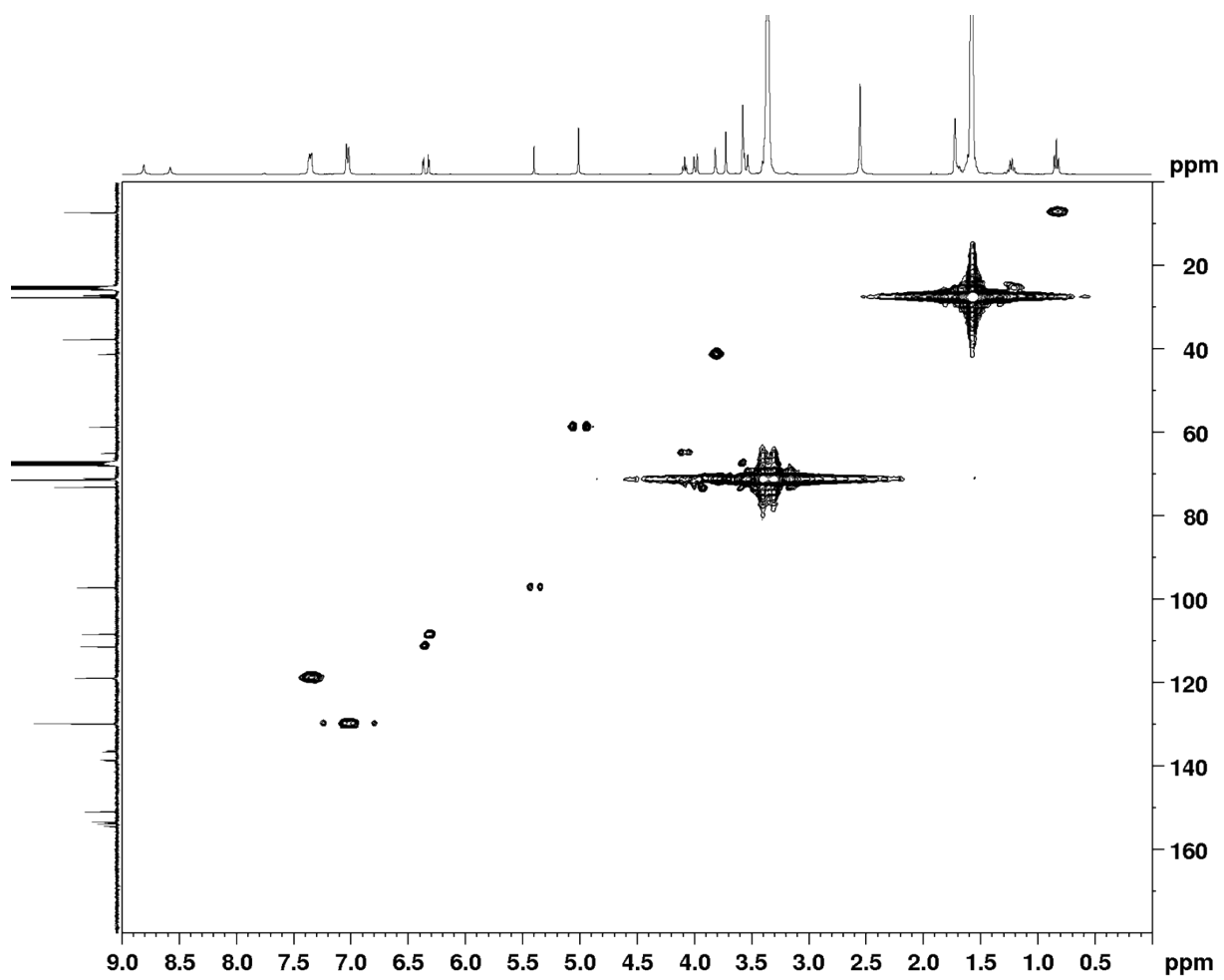


Figure S15. HMQC spectrum of PAU-25.

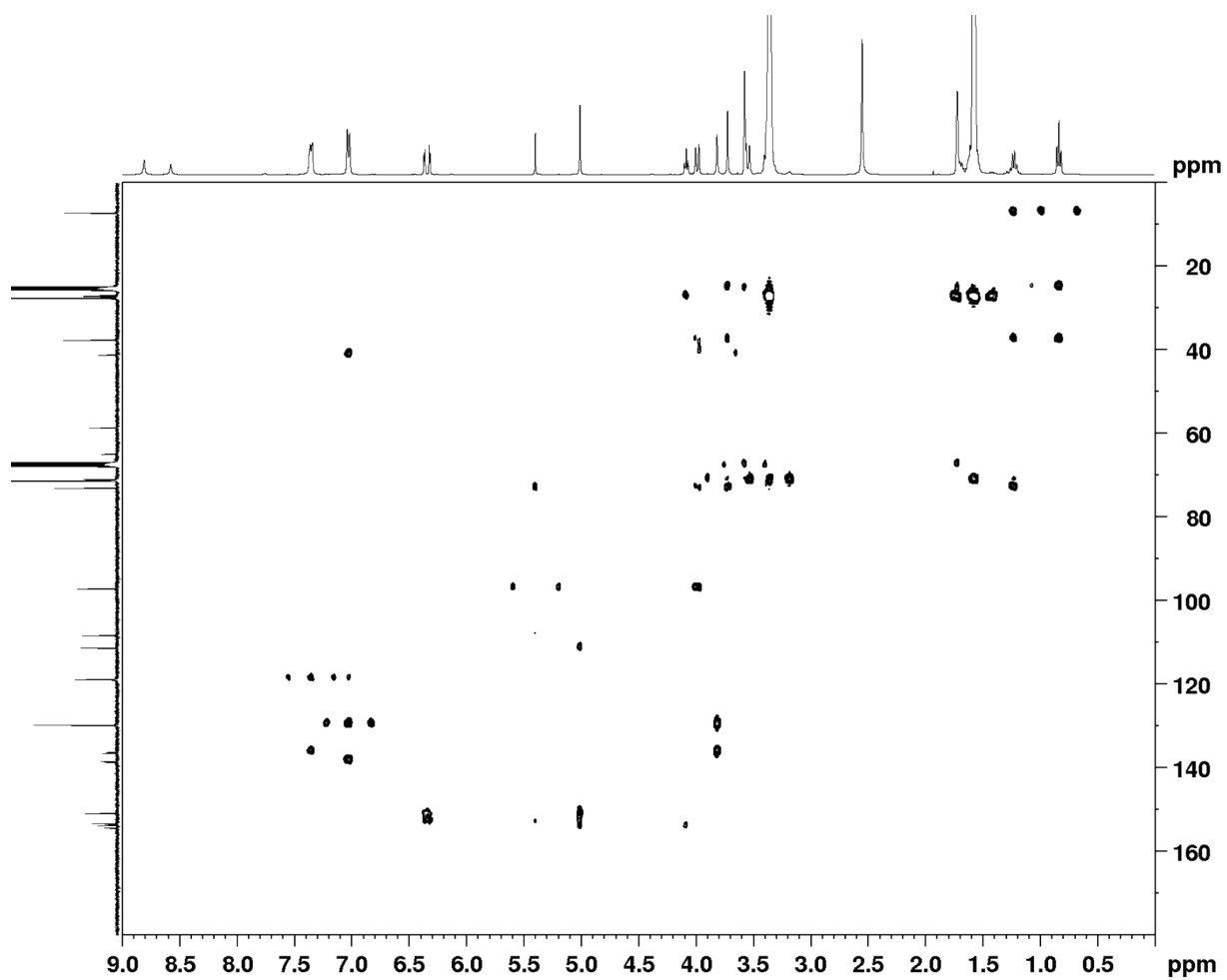


Figure S16. HMBC spectrum of PAU-25.

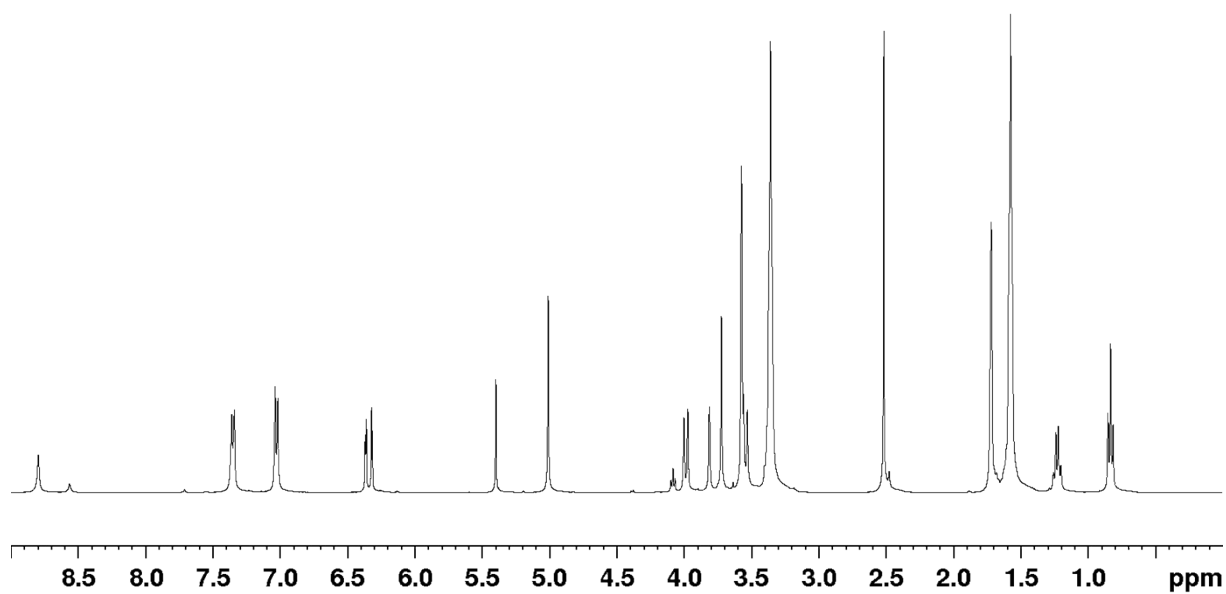


Figure S17. ^1H NMR spectrum of PAU-51.

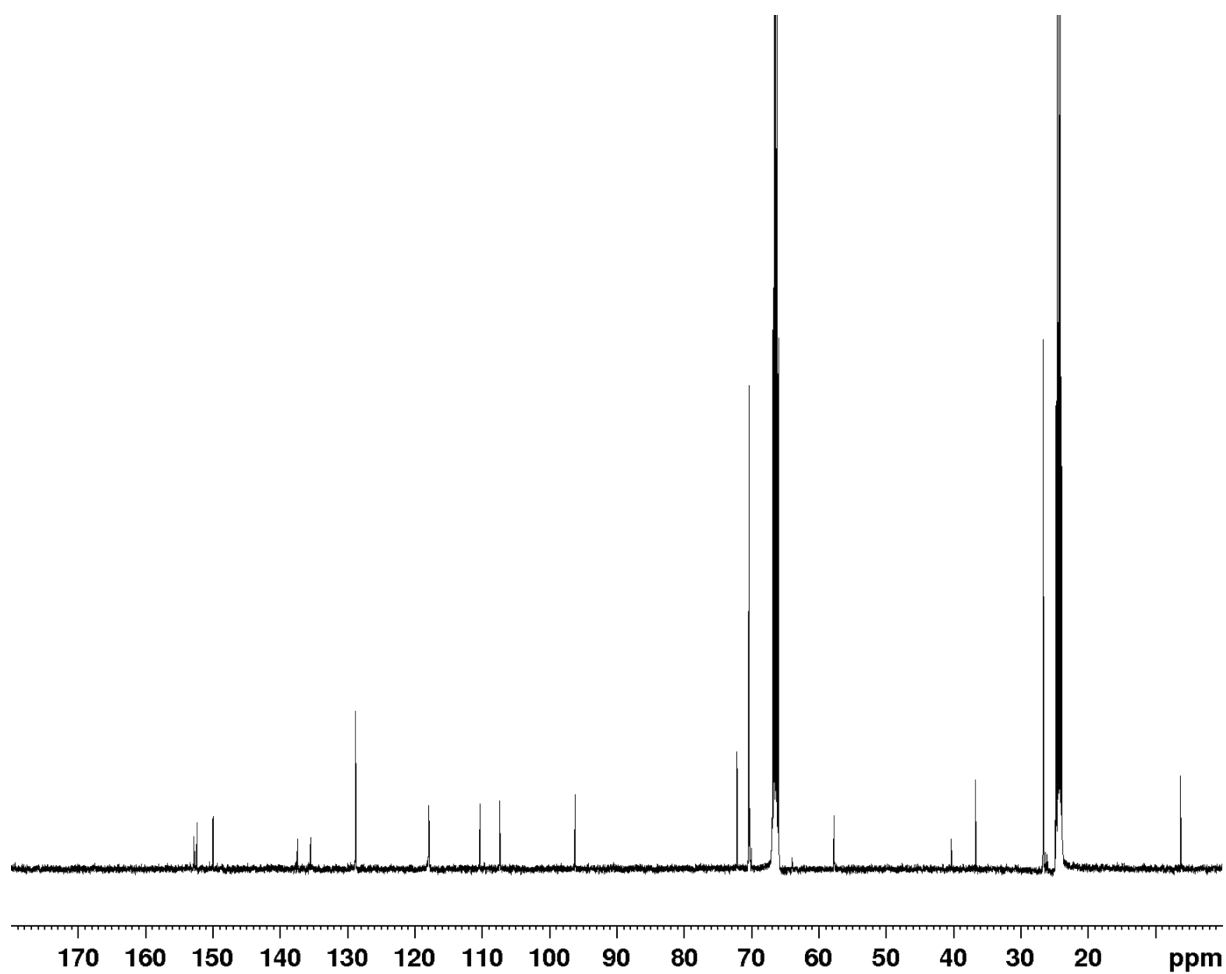


Figure S18. ^{13}C NMR spectrum of PAU-51.

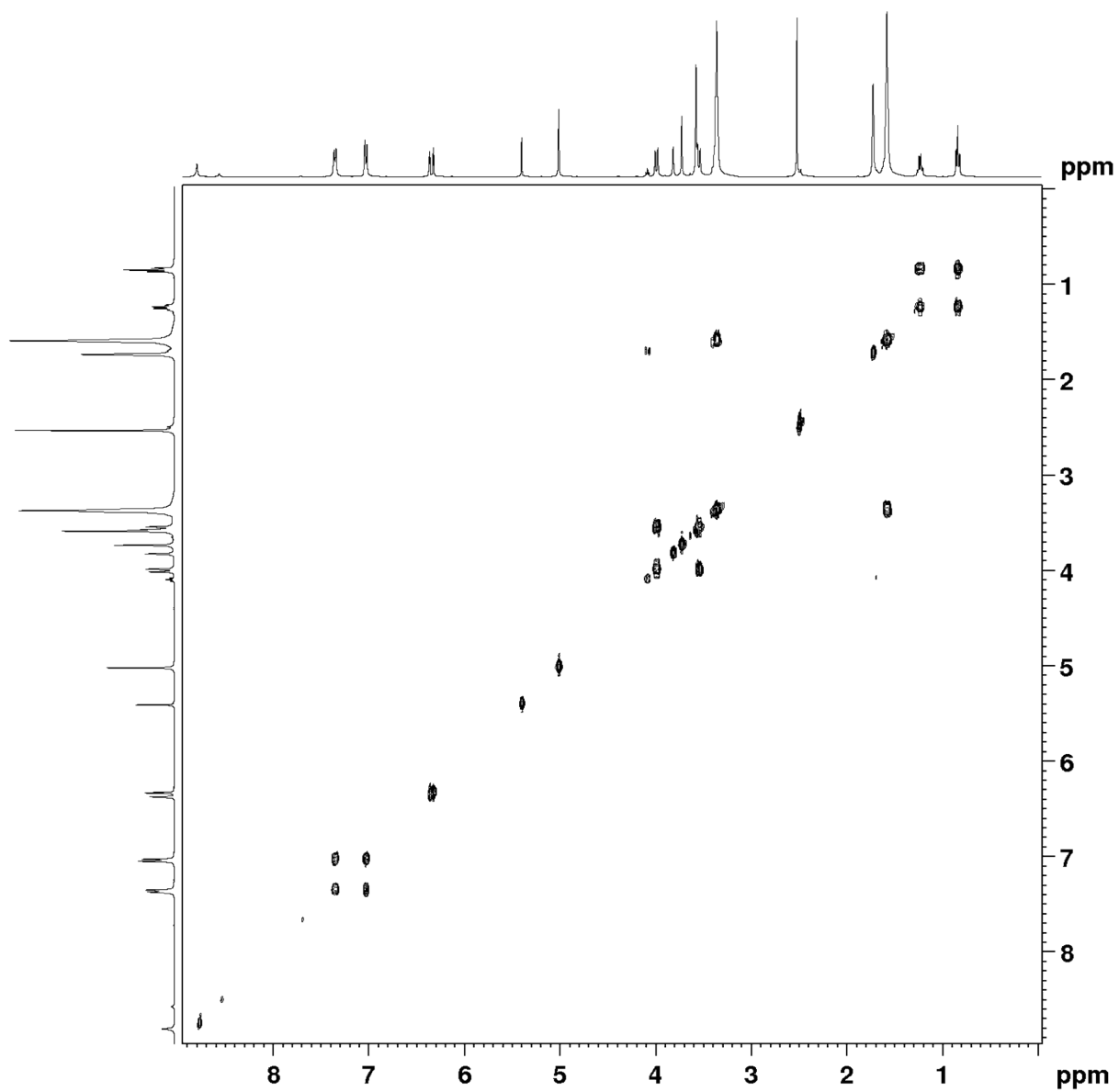


Figure S19. COSY spectrum of PAU-51.

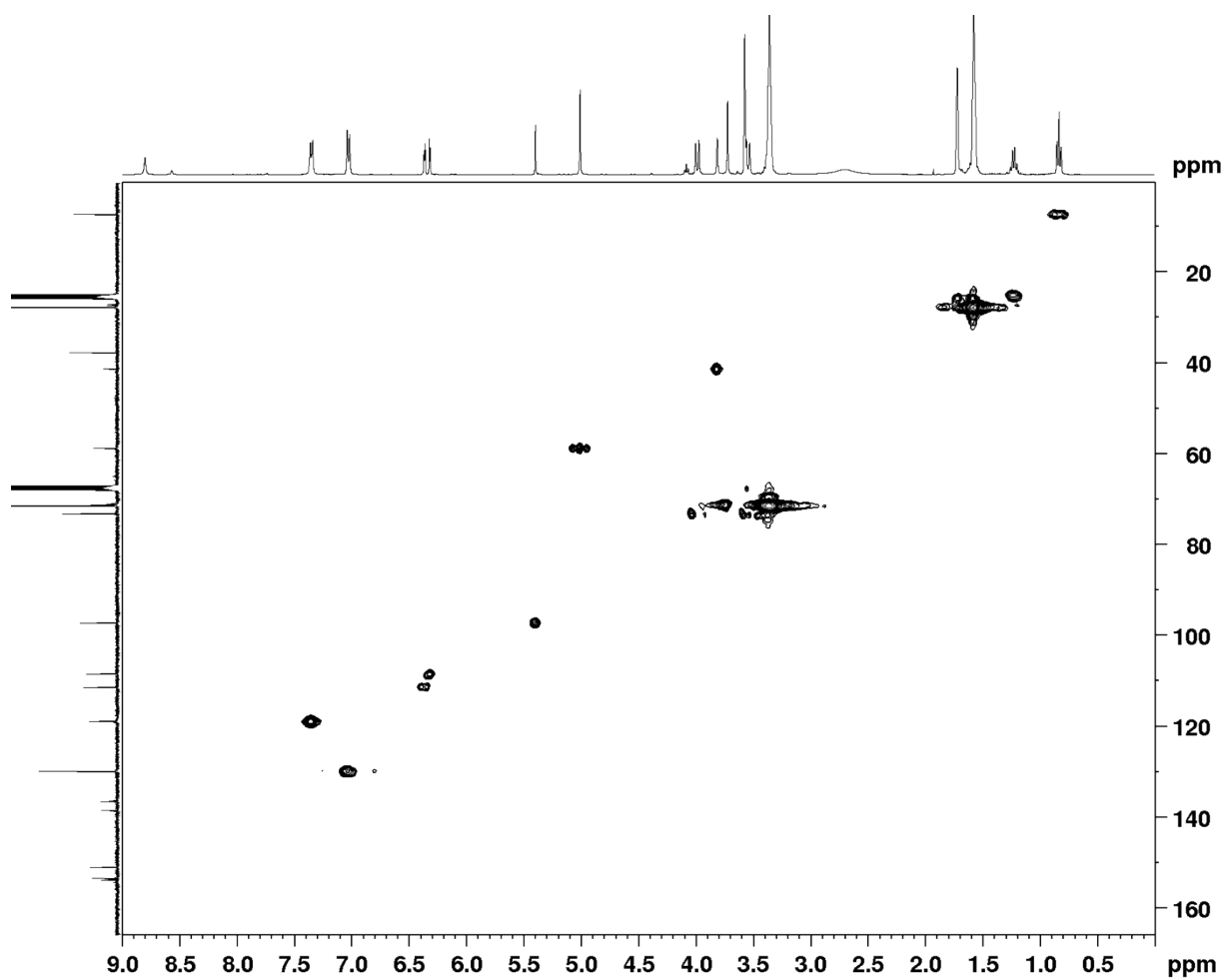


Figure S20. HMQC spectrum of PAU-51.

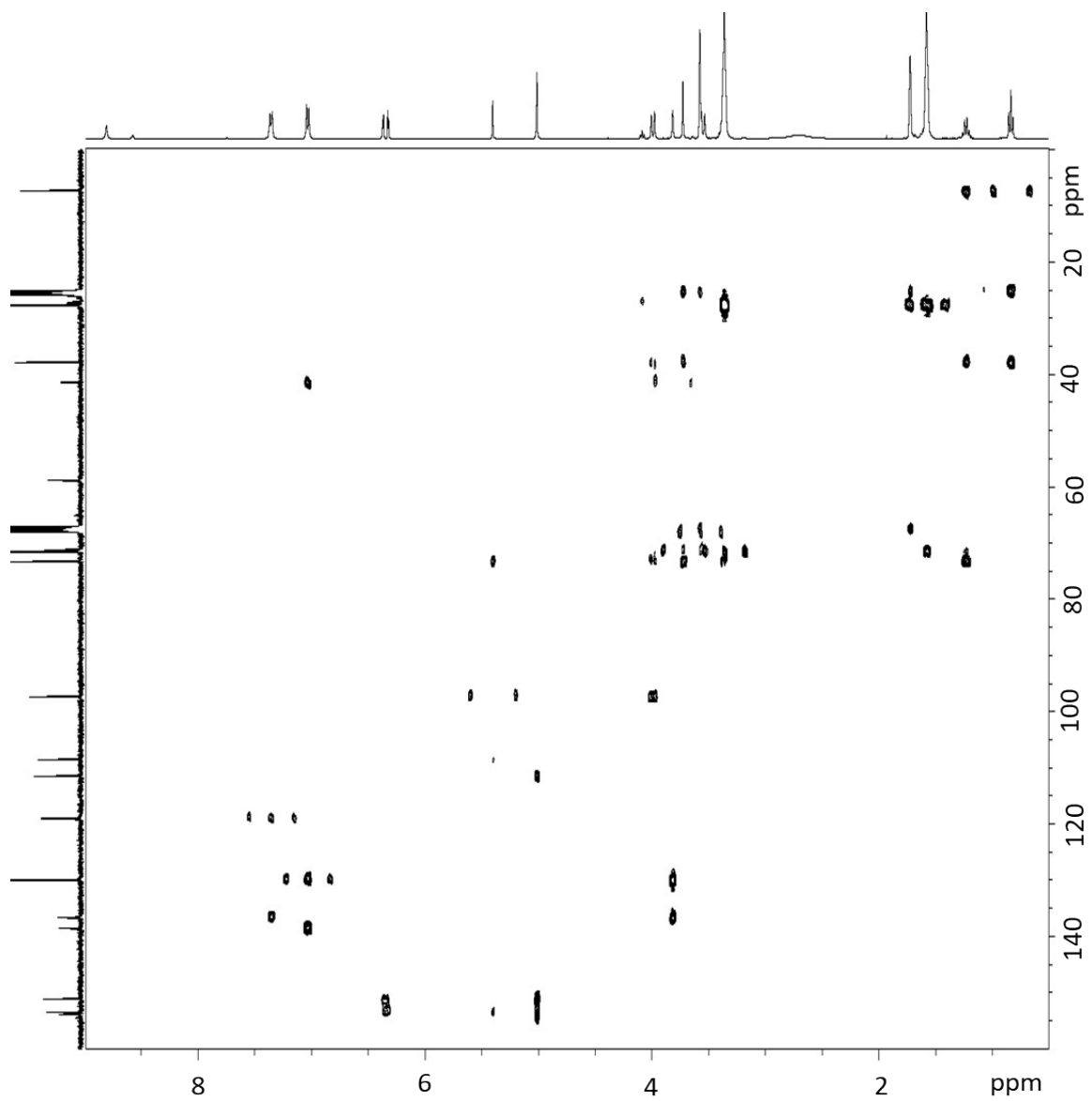


Figure S21. HMBC spectrum of PAU-51.

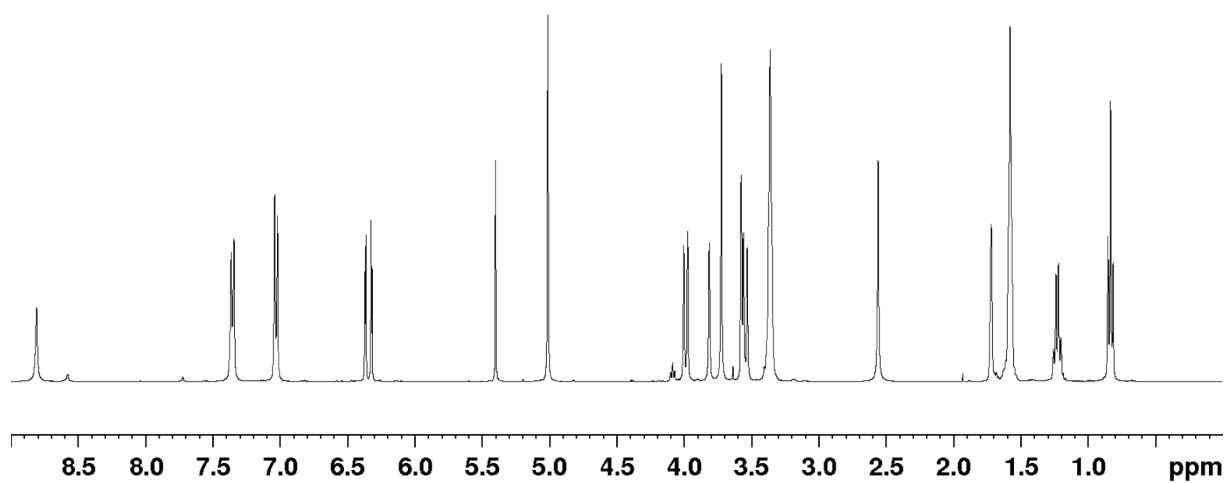


Figure S22. ^1H NMR spectrum of PAU-71.

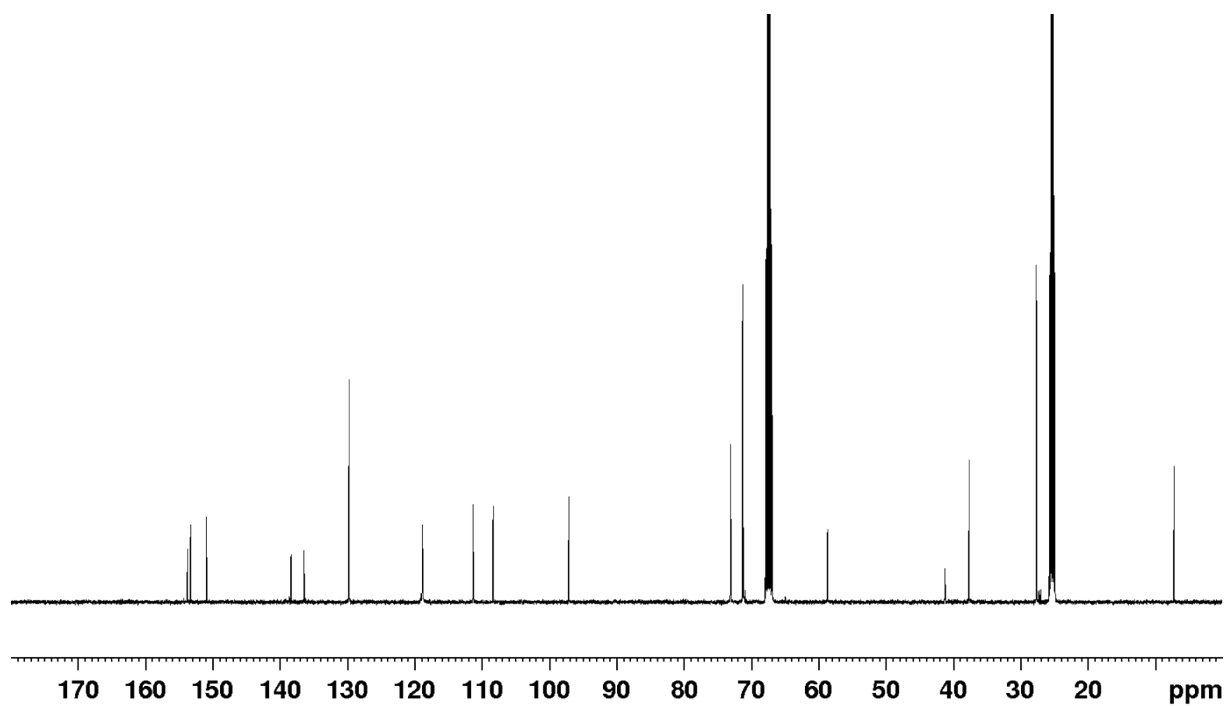


Figure S23. ^{13}C NMR spectrum of PAU-71.

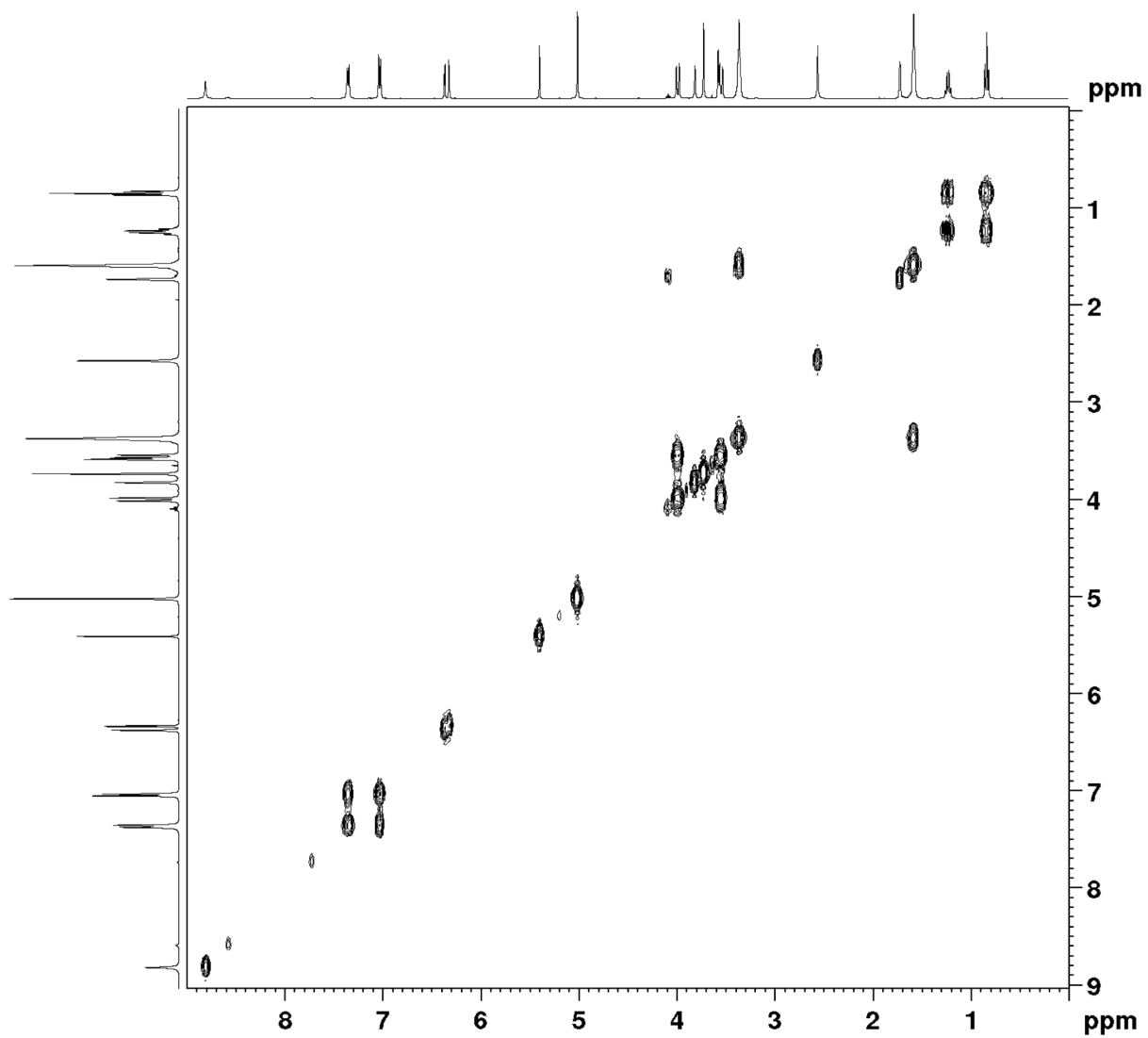


Figure S24. COSY spectrum of PAU-71.

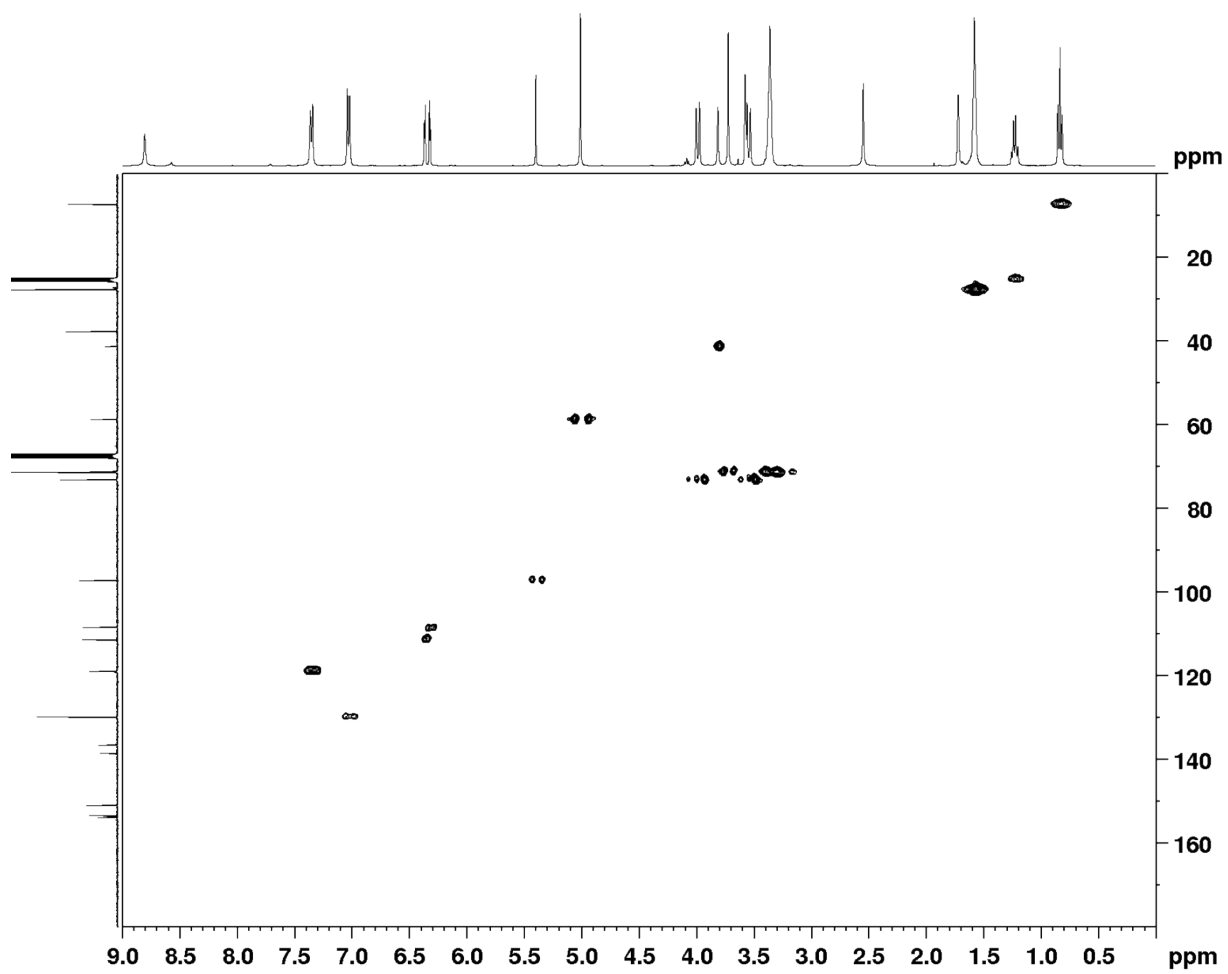


Figure S25. HMQC spectrum of PAU-71.

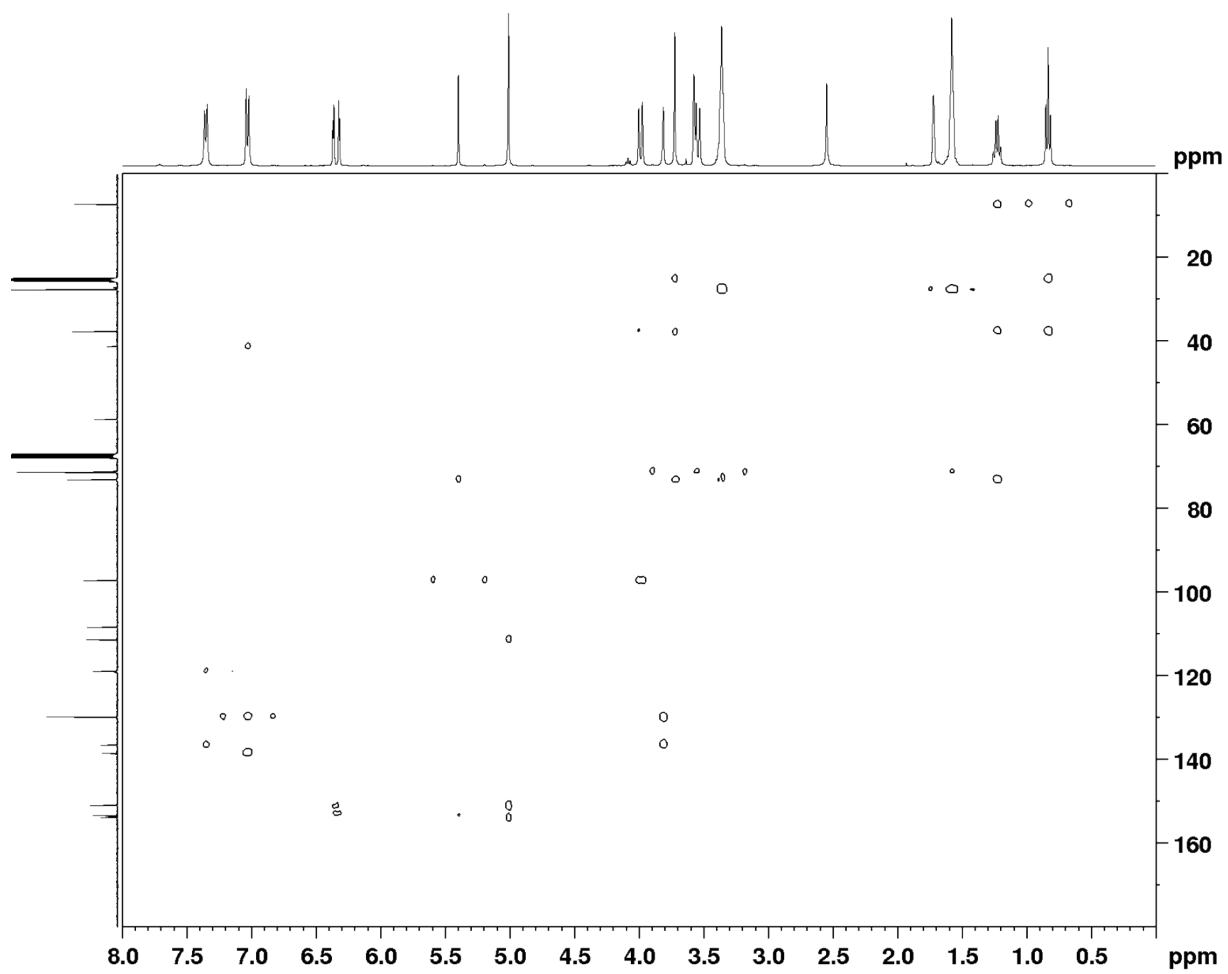


Figure S26. HMBC spectrum of PAU-71.

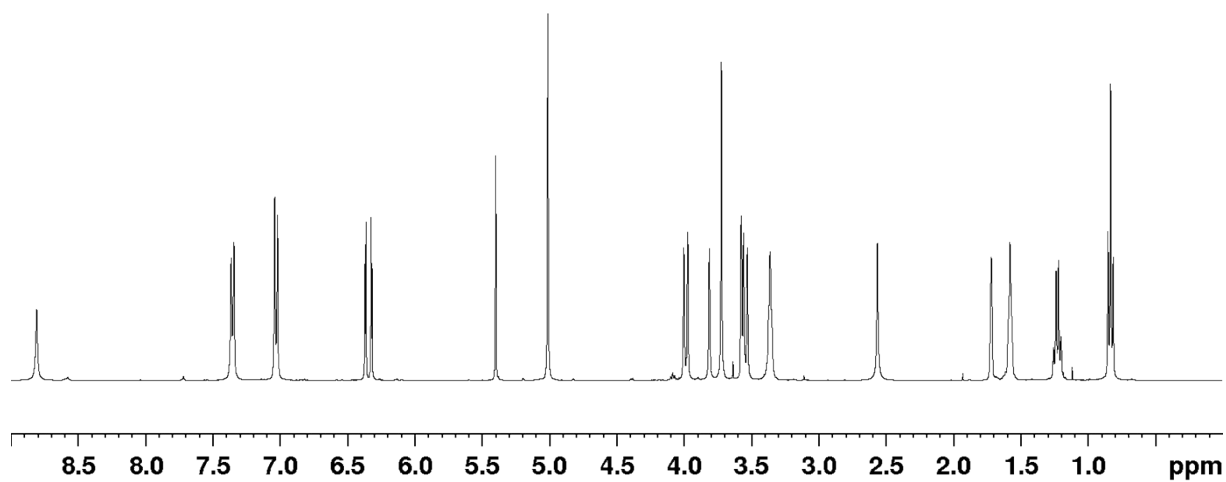


Figure S27. ^1H NMR spectrum of PAU-86.

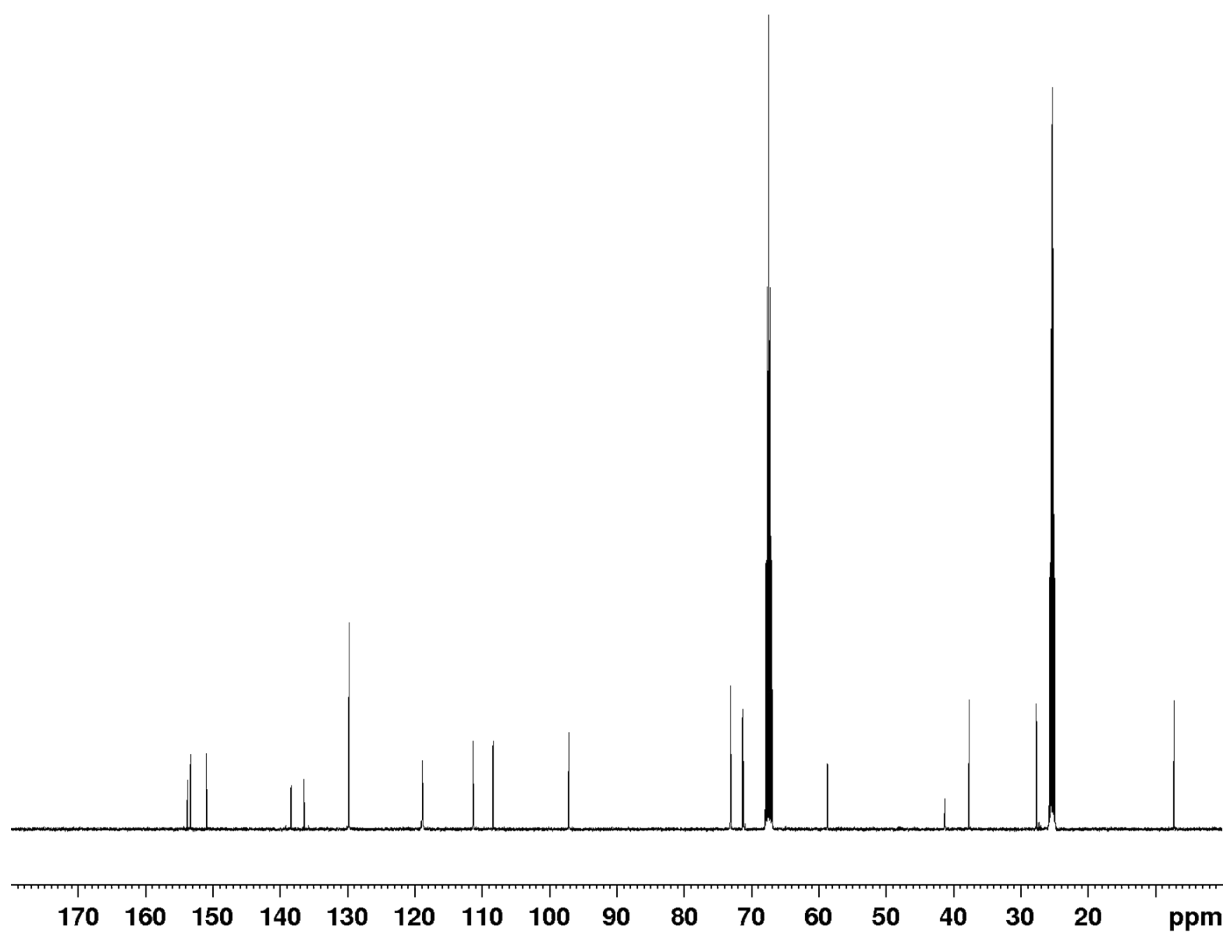


Figure S28. ^{13}C NMR spectrum of PAU-86.

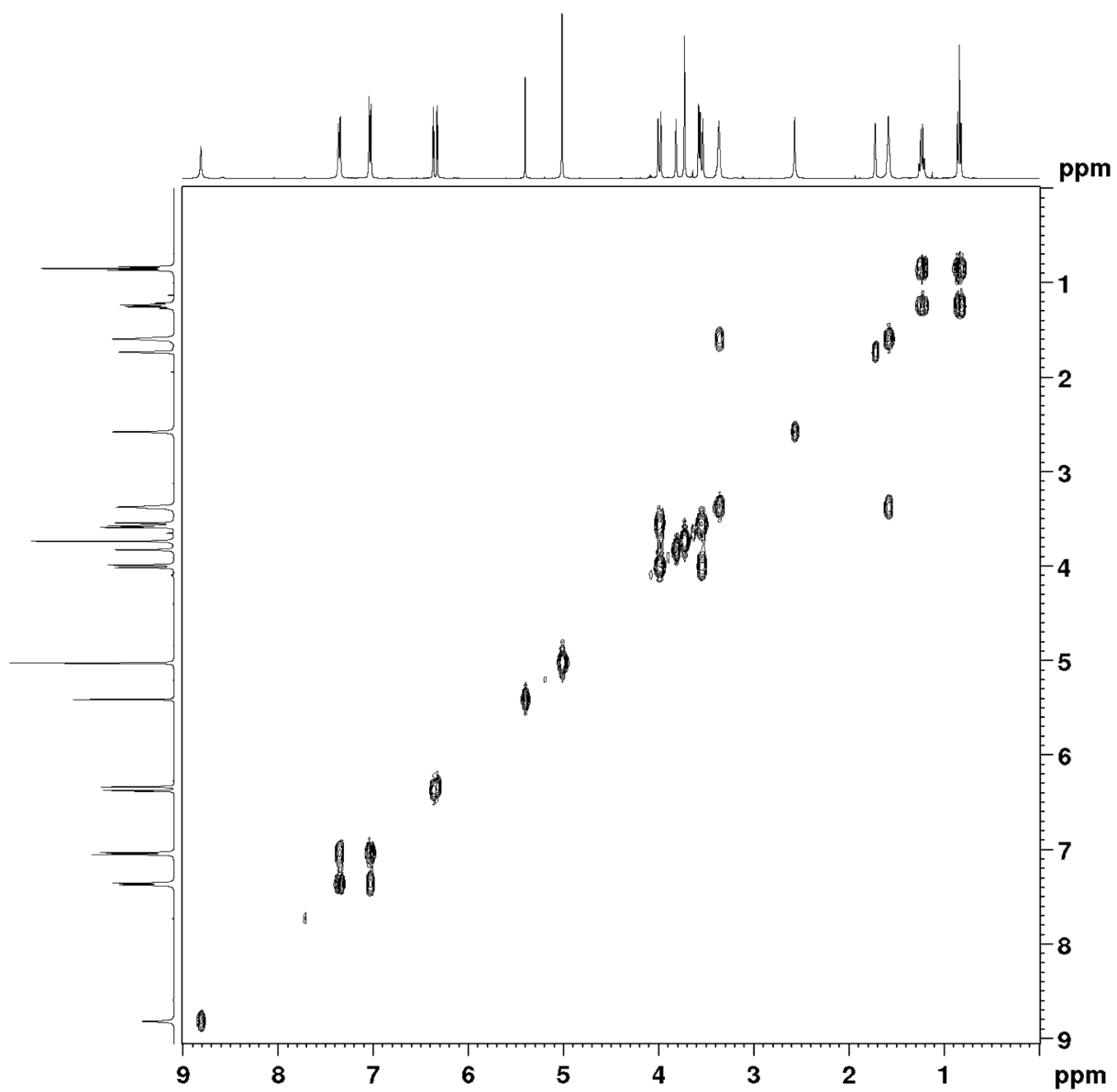


Figure S29. COSY spectrum of PAU-86.

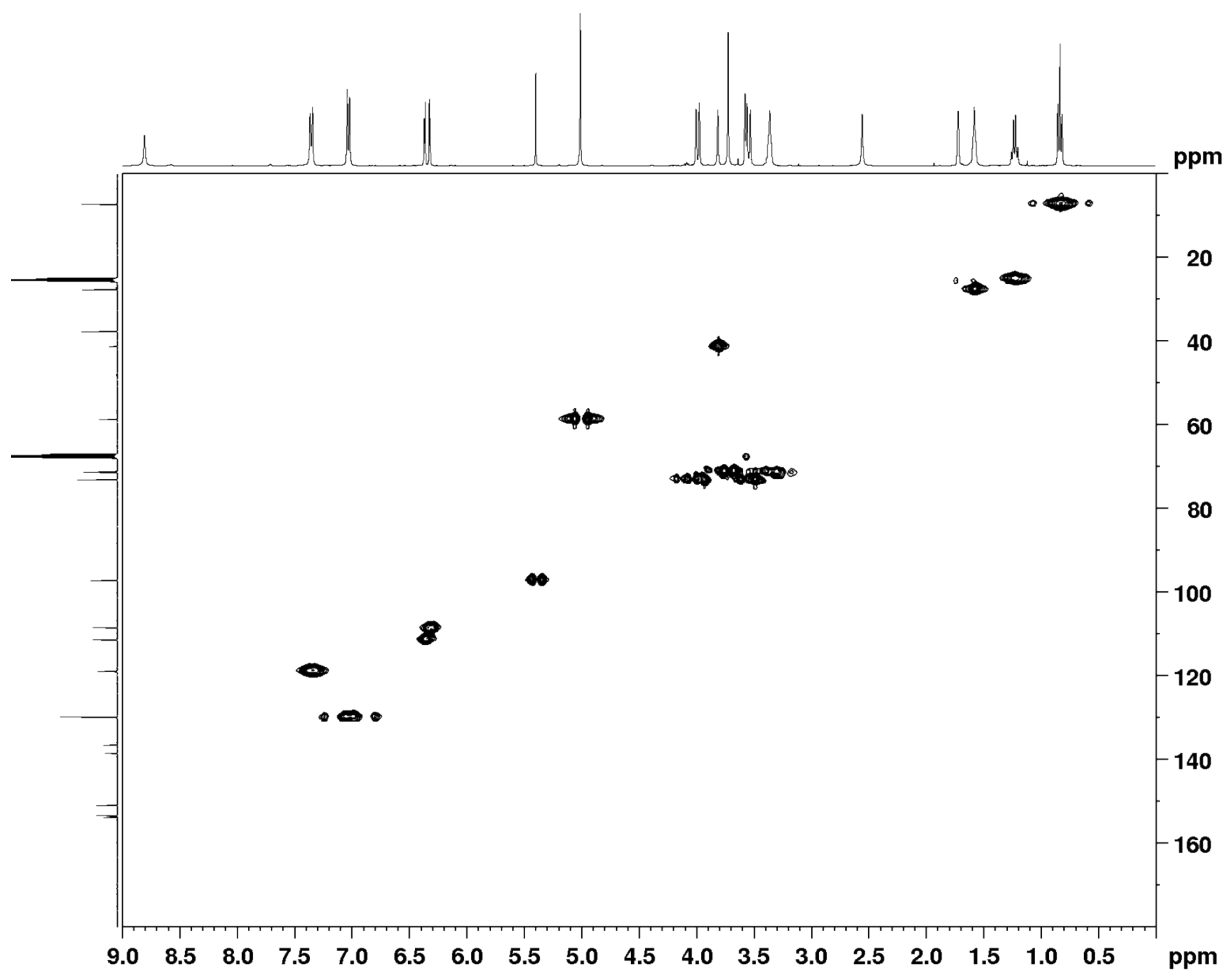


Figure S30. HMQC spectrum of PAU-86.

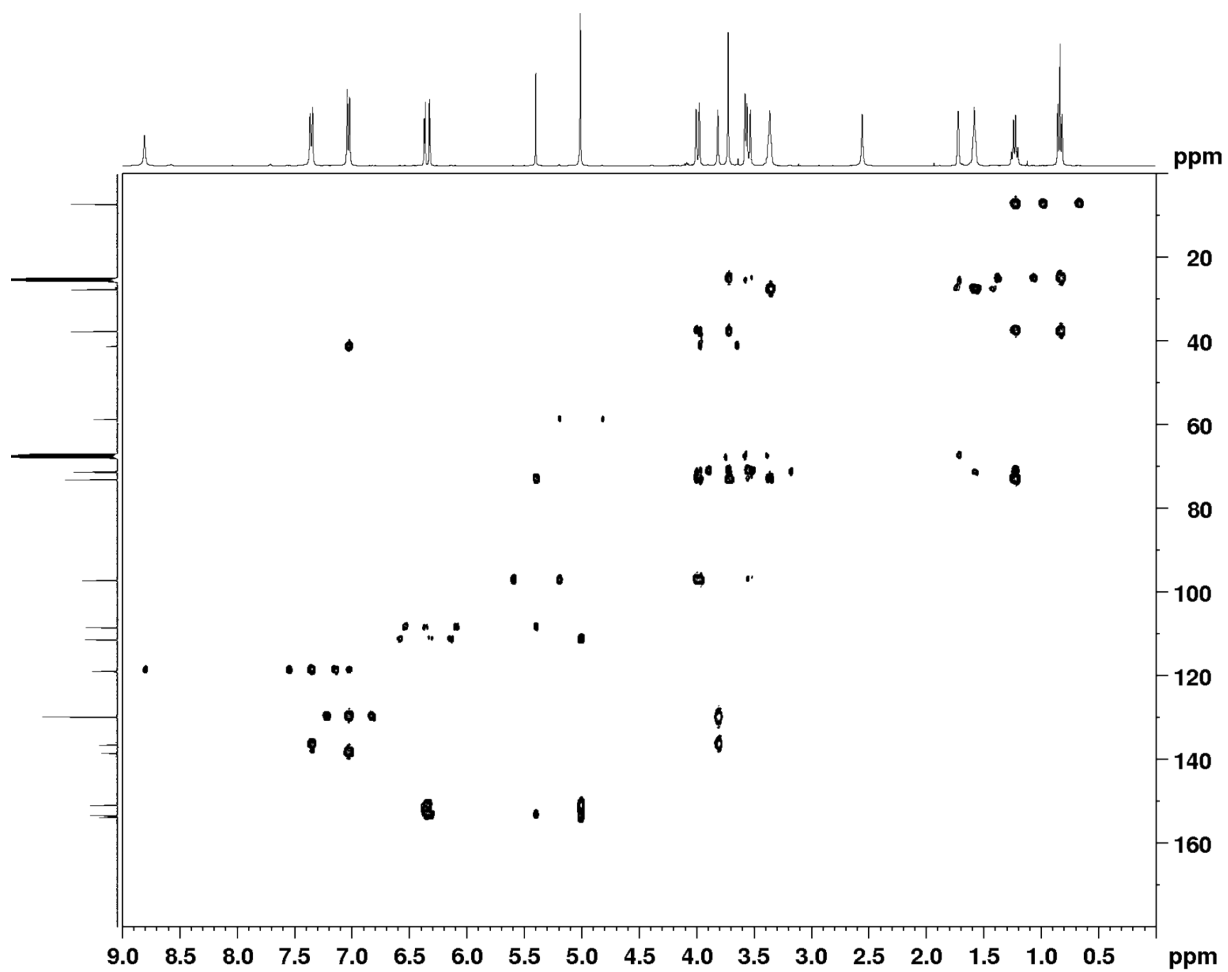


Figure S31. HMBC spectrum of PAU-86.

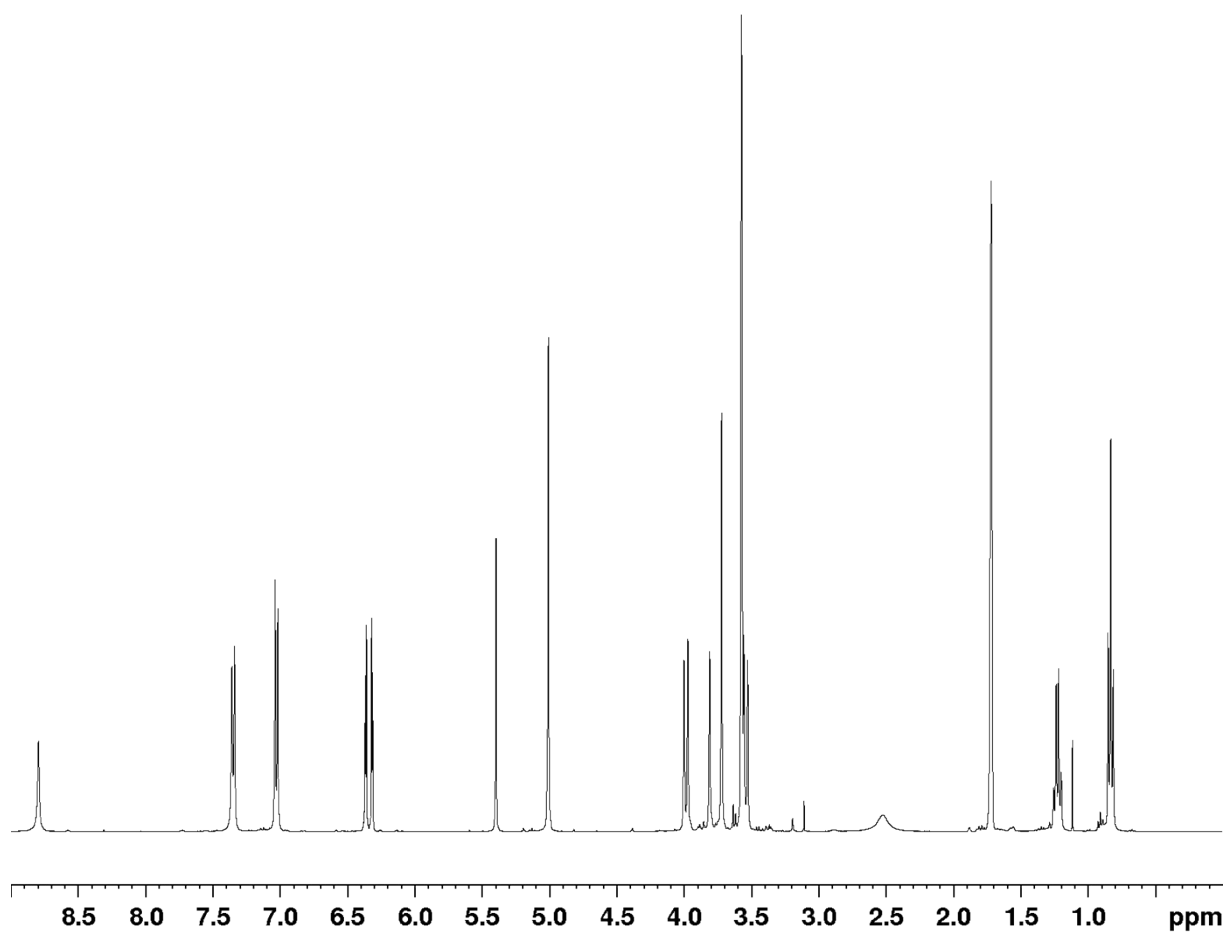


Figure S32. ^1H NMR spectrum of PAU-MDI.

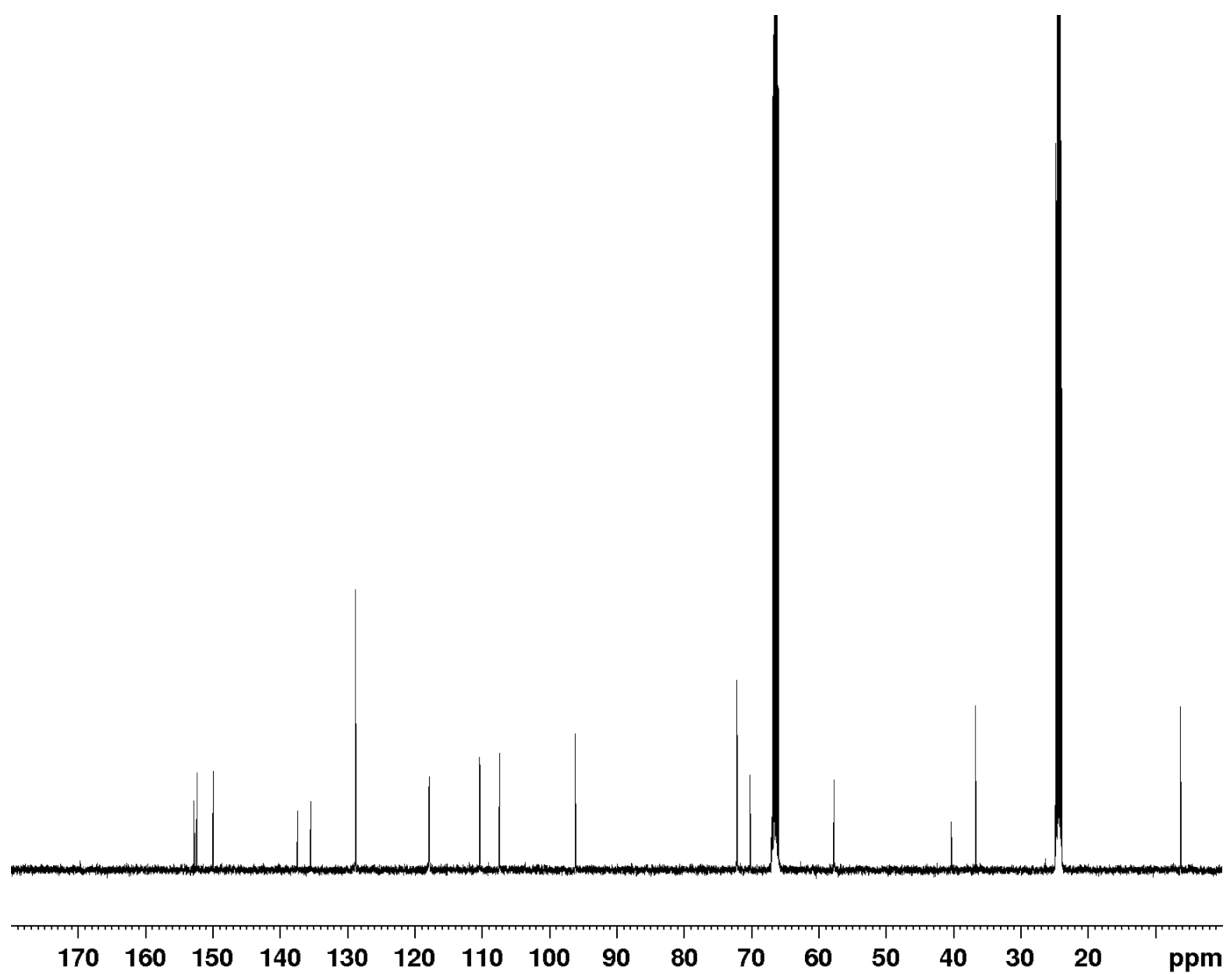


Figure S33. ^{13}C NMR spectrum of PAU-MDI.

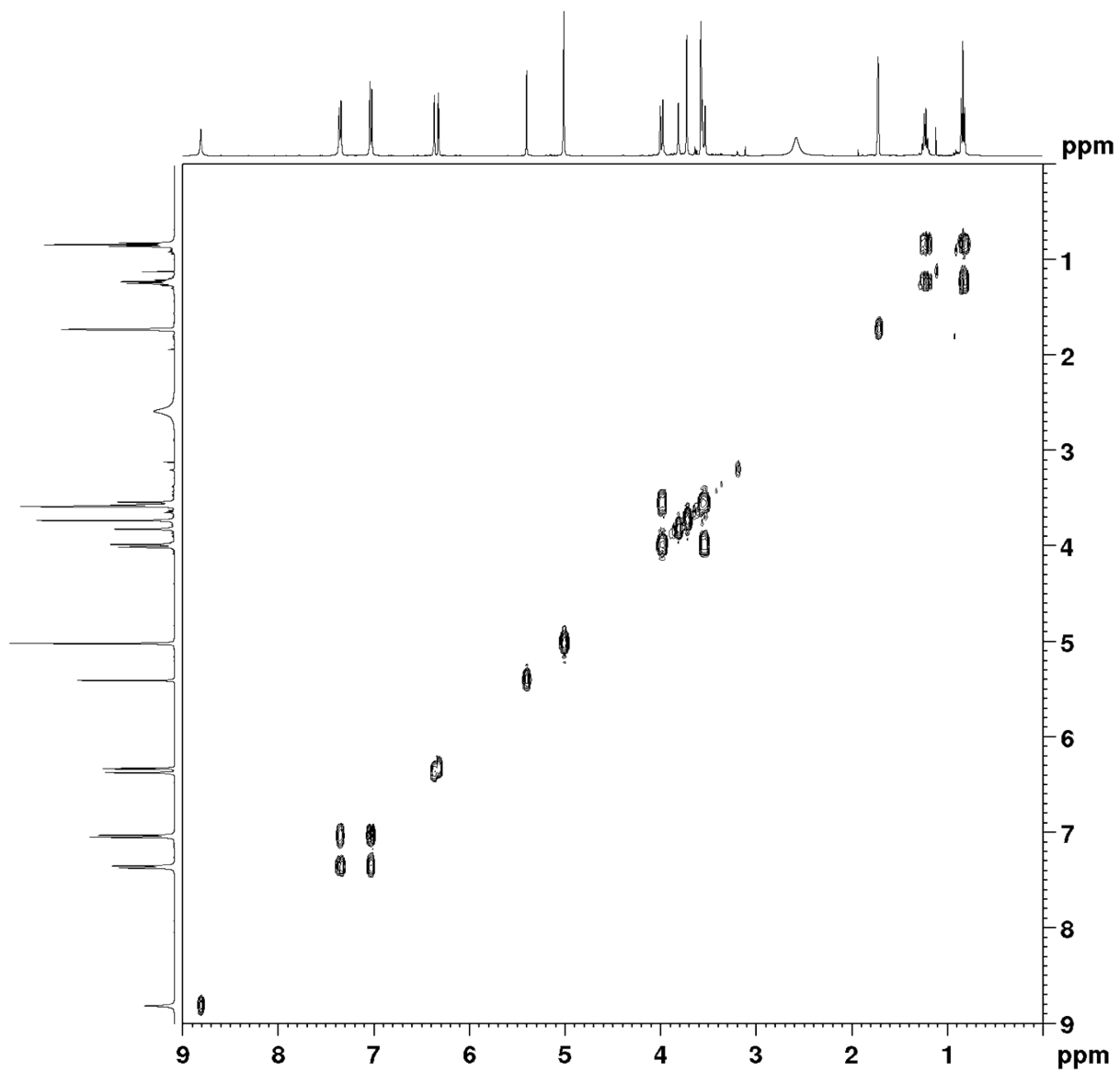


Figure S34. COSY spectrum of PAU-MDI.

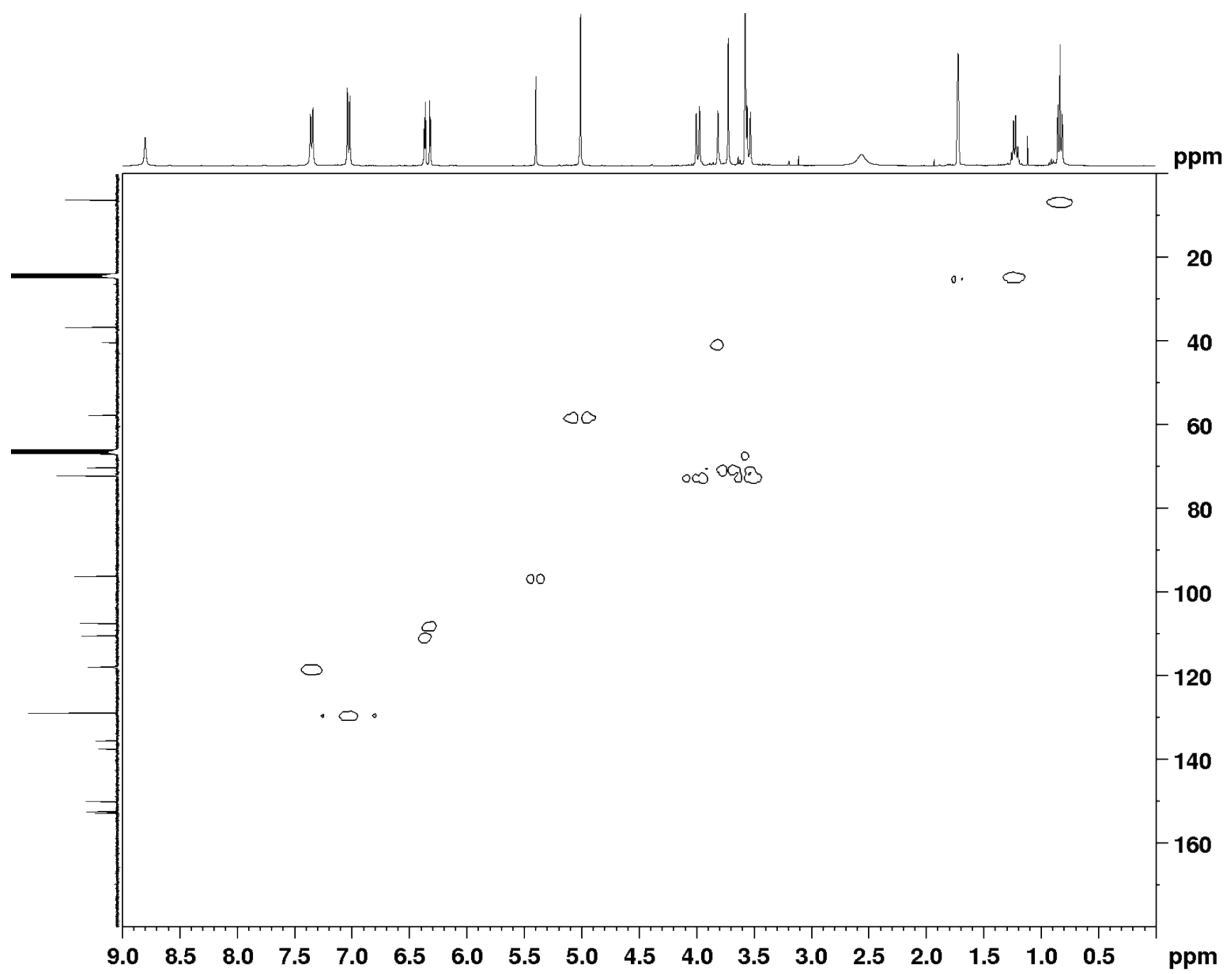


Figure S35. HMQC spectrum of PAU-MDI.

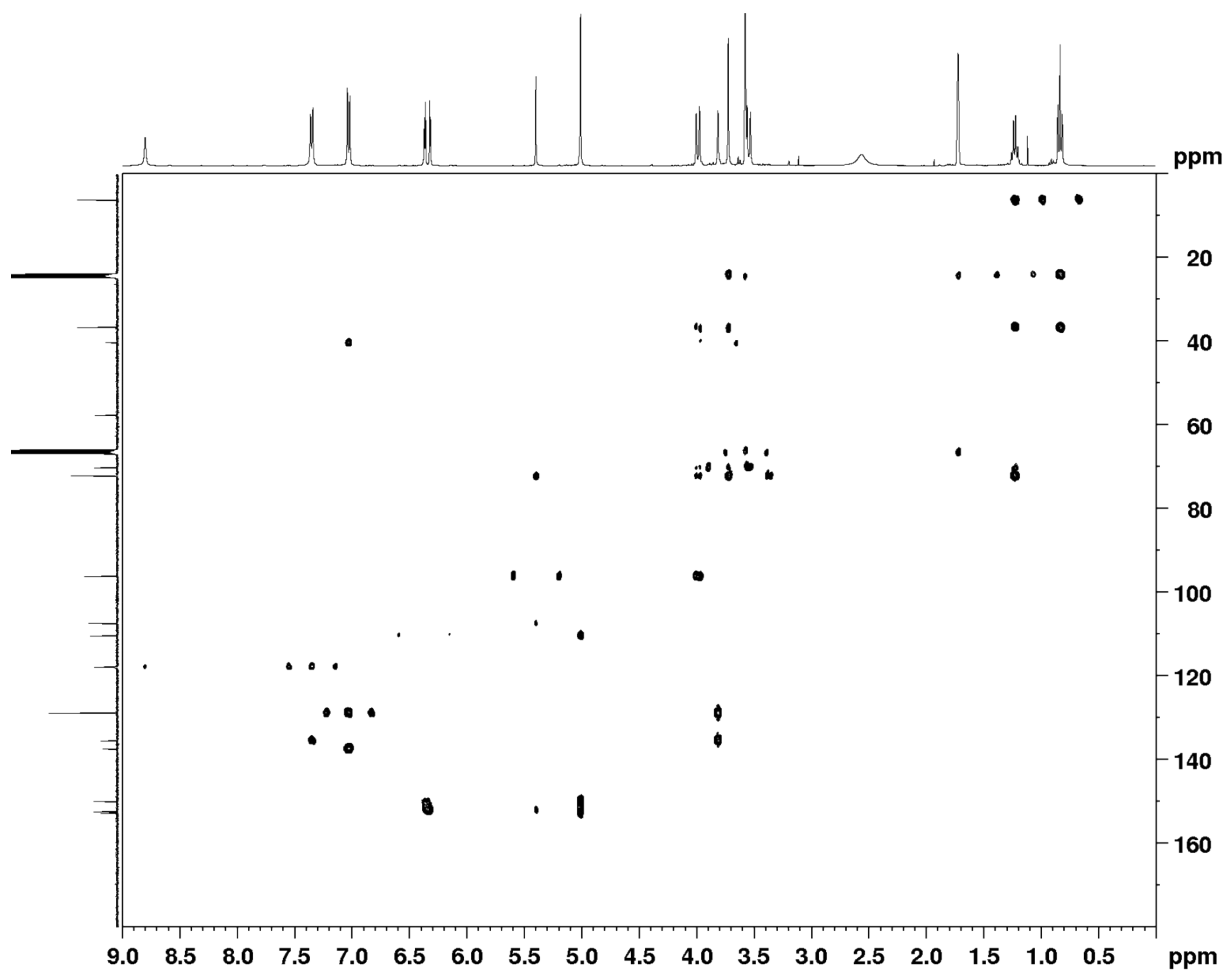


Figure S36. HMBC spectrum of PAU-MDI.

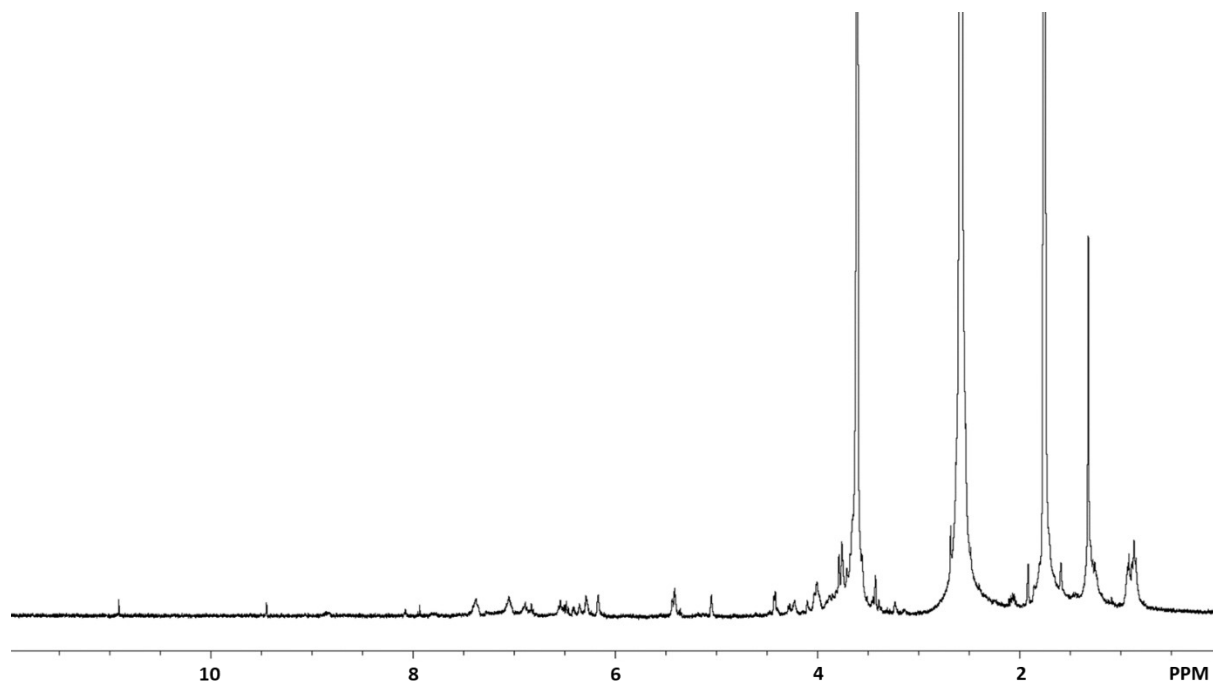


Figure S37. ^1H NMR spectrum of the soluble fraction of PU-MDI after TGA measurements.

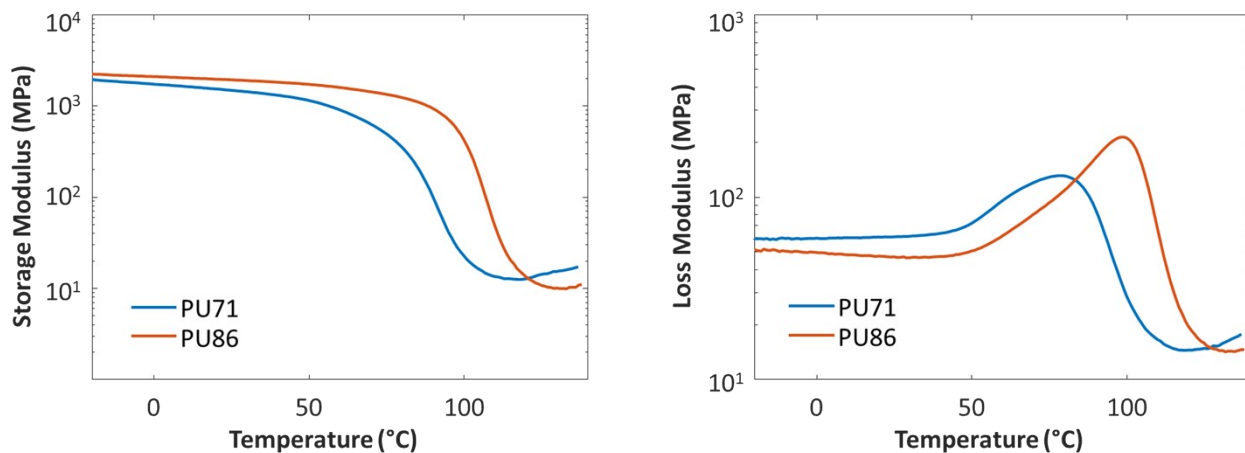


Figure S38. Temperature sweep DMA (left: storage moduli, and right: loss moduli) curves of PAU-71 and PAU-86.

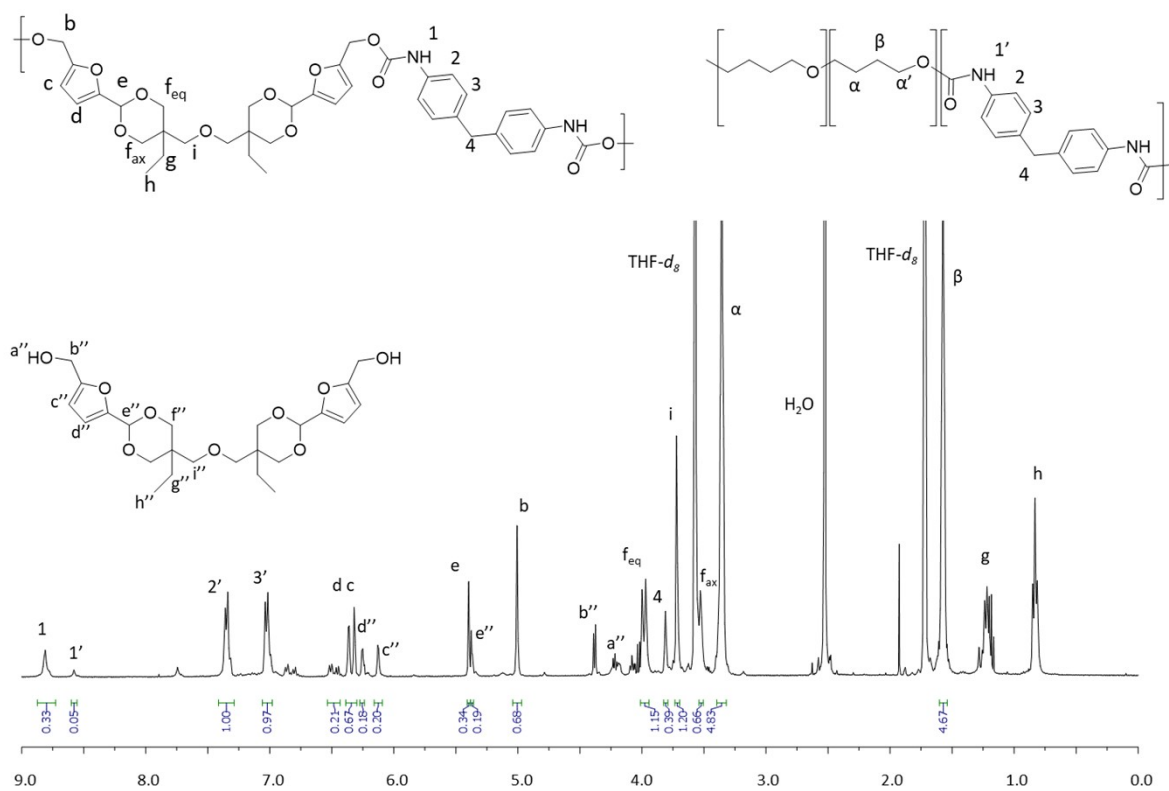


Figure S39. ^1H NMR spectrum of PAU-86 after the rheology measurements.

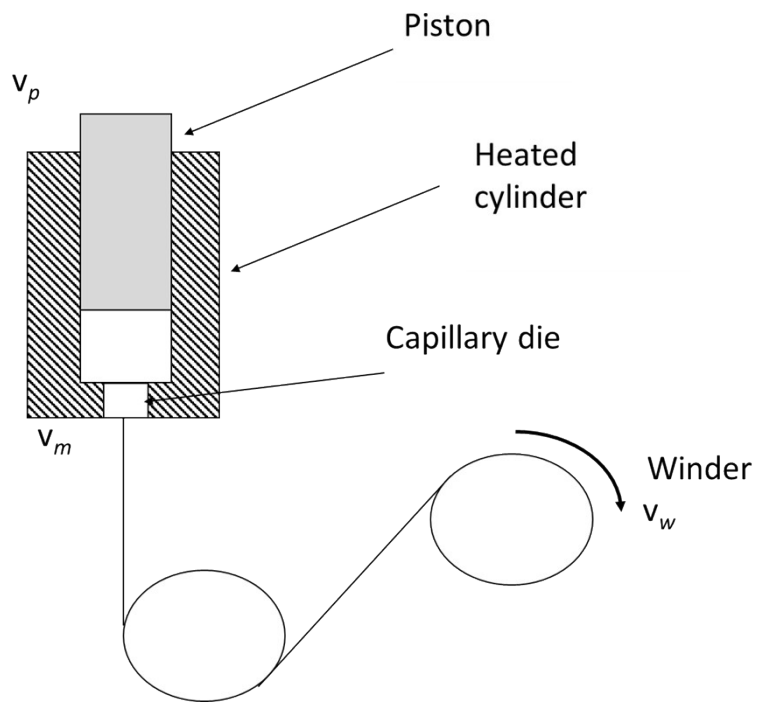


Figure S40. Schematic representation of melt-spinning process.

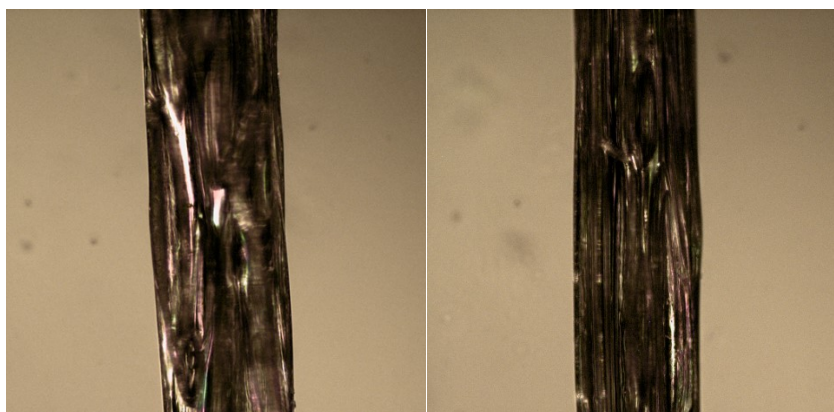


Figure S41. Cross-polarized optical microscopy images of the melt-spun PAU-86 fibre at the beginning of the spinning procedure (left) and at the end of it (right).

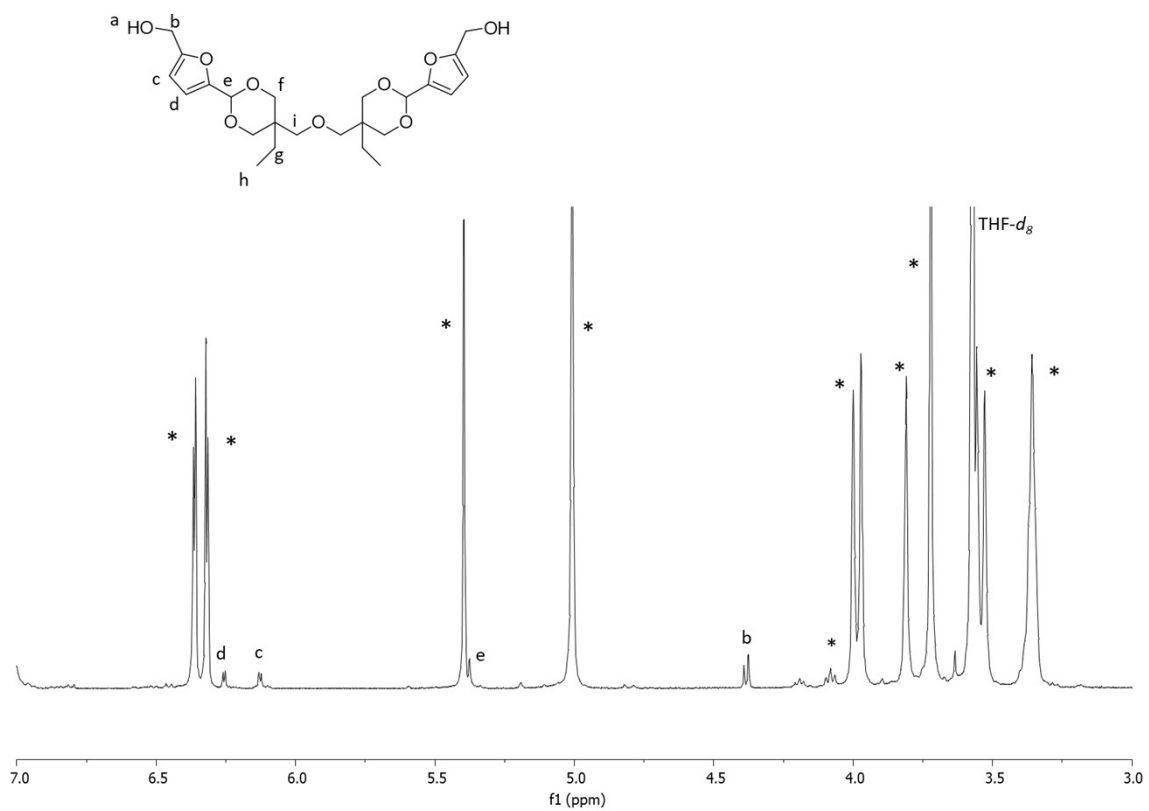


Figure S42. $^1\text{H-NMR}$ of PAU-86 fibre. The signals corresponded to Monomer T were indicated. The signals corresponding to PAU-86 were marked by stars (*). For specific assignments, please see Fig. 1.



Figure S43. PAU-85 before fibre spinning.

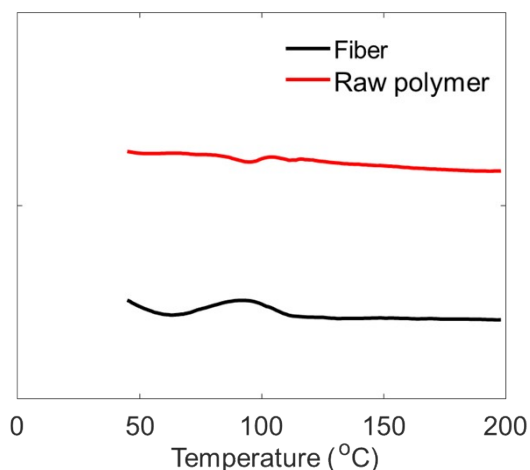


Figure S44. First heating cycle of PAU-86 fibre (black curve) and raw polymer powder before processing (red curve).

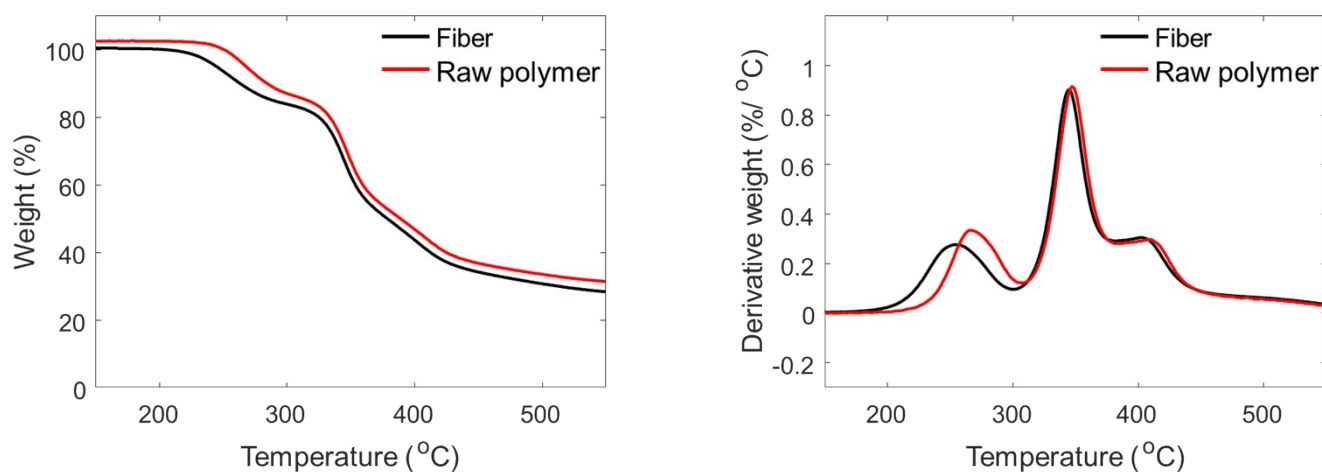


Figure S45. TGA (left) weight loss and (right) derivative weight loss curves of PAU-86 fibre (black curve) and unprocessed polymer powder (red curve).

Table S1. Thermal properties of PU86 before and after fiber spinning. ^a The temperature for maximal degradation rate in TGA. ^b The temperature for 5% weight loss in TGA curves.

	T_d^a (°C)	T_5^b (°C)
PU86-fiber	255, 346, 404	244
PU86-raw	266, 349, 411	268

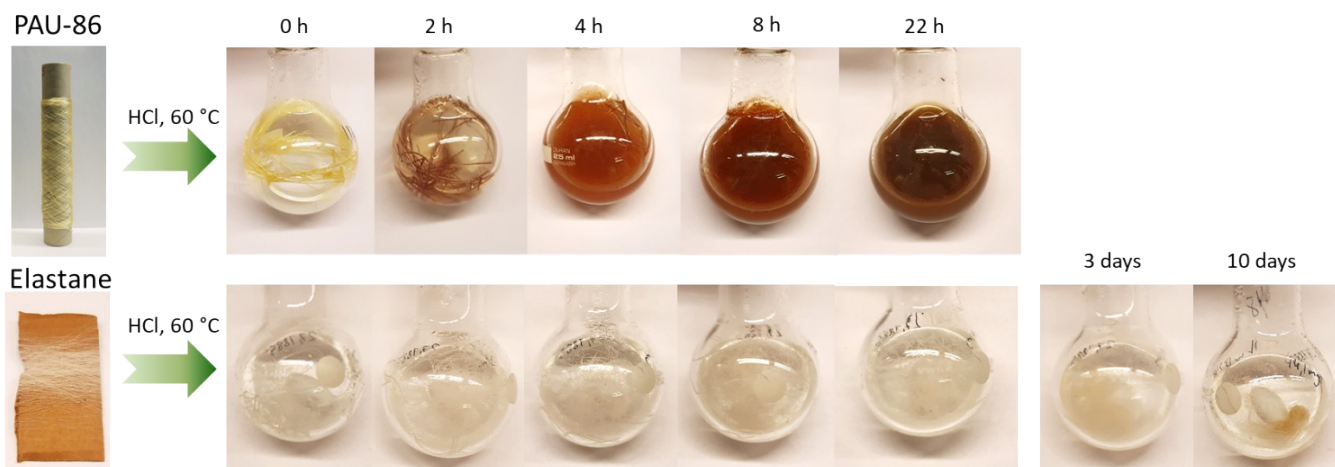


Figure S46. Acid-hydrolysis of the PAU-86 fibre and Elastane. The time above each photo indicates the reaction time when the photo was taken.

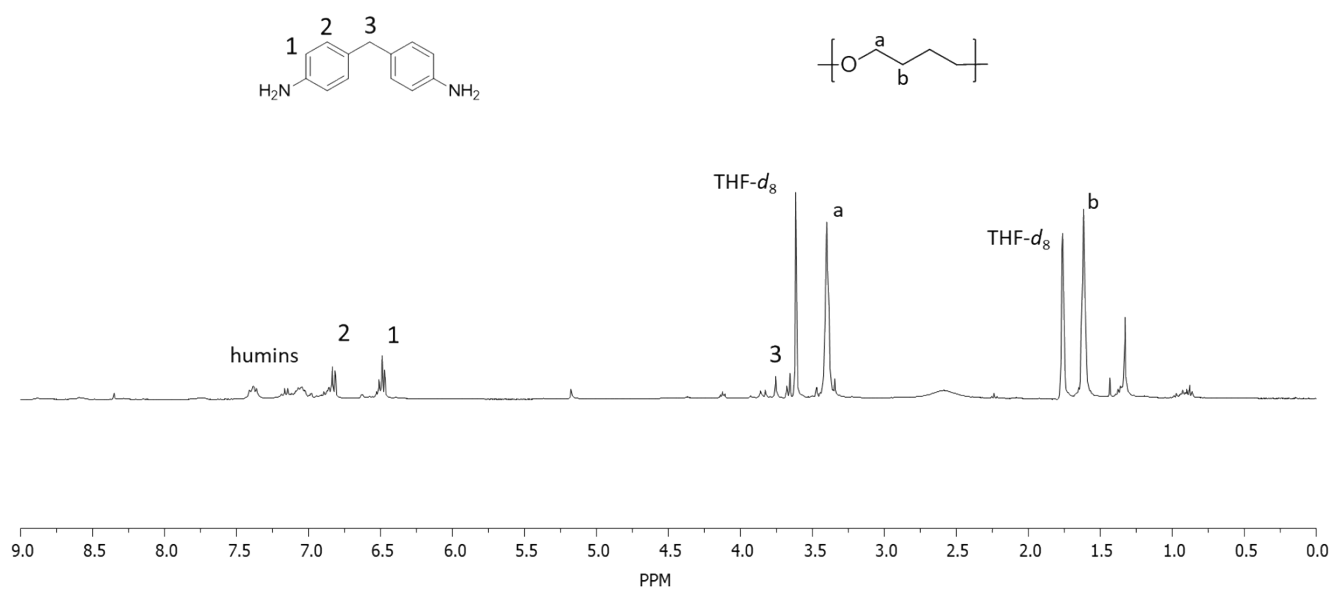


Figure S47. ^1H NMR spectrum in $\text{THF-}d_8$ of yielded material extracted by THF from the solid residue remaining of the PAU-86 fibre.

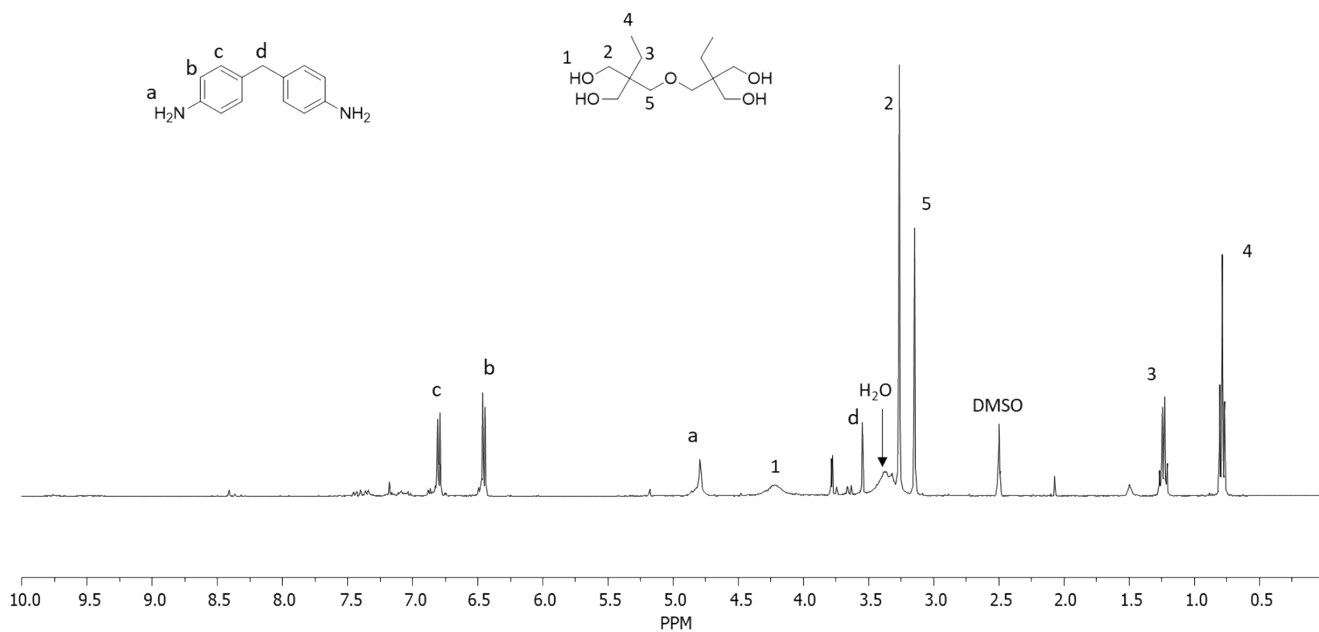


Figure S48. ^1H NMR spectrum in DMSO-d_6 of yielded material after hydrolysis of PAU-86 fibre for 24 h. The signals for di-TMP and 4,4-diaminodiphenylmethane were indicated.

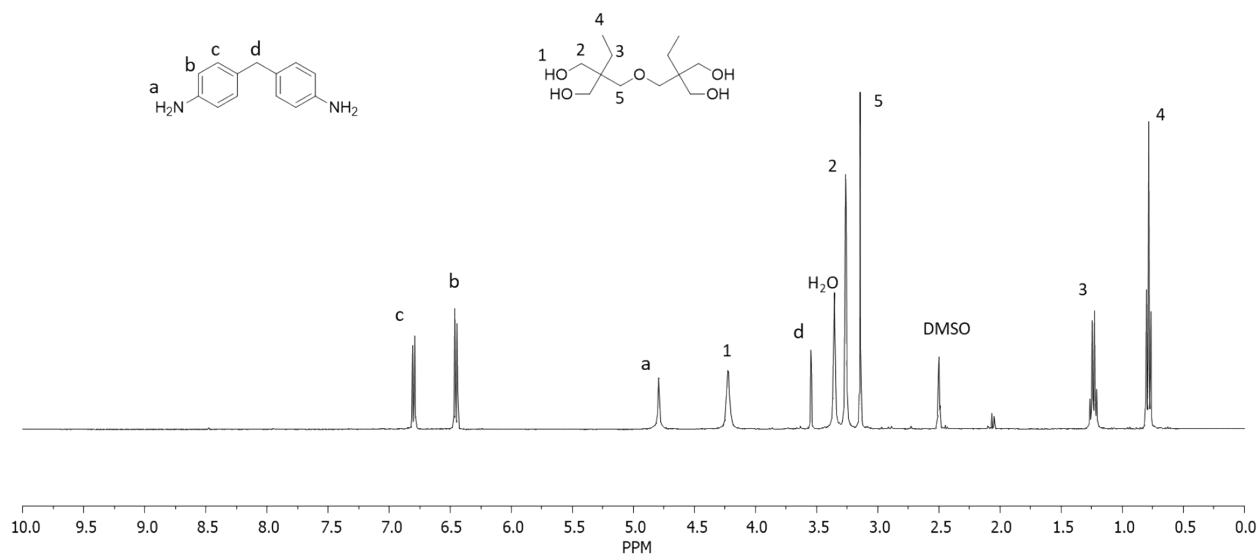


Figure S49. ^1H NMR spectrum in DMSO-d_6 of yielded material after hydrolysis of PAU-86 fibre for 48 h. The signals for di-TMP and 4,4-diaminodiphenylmethane were indicated.

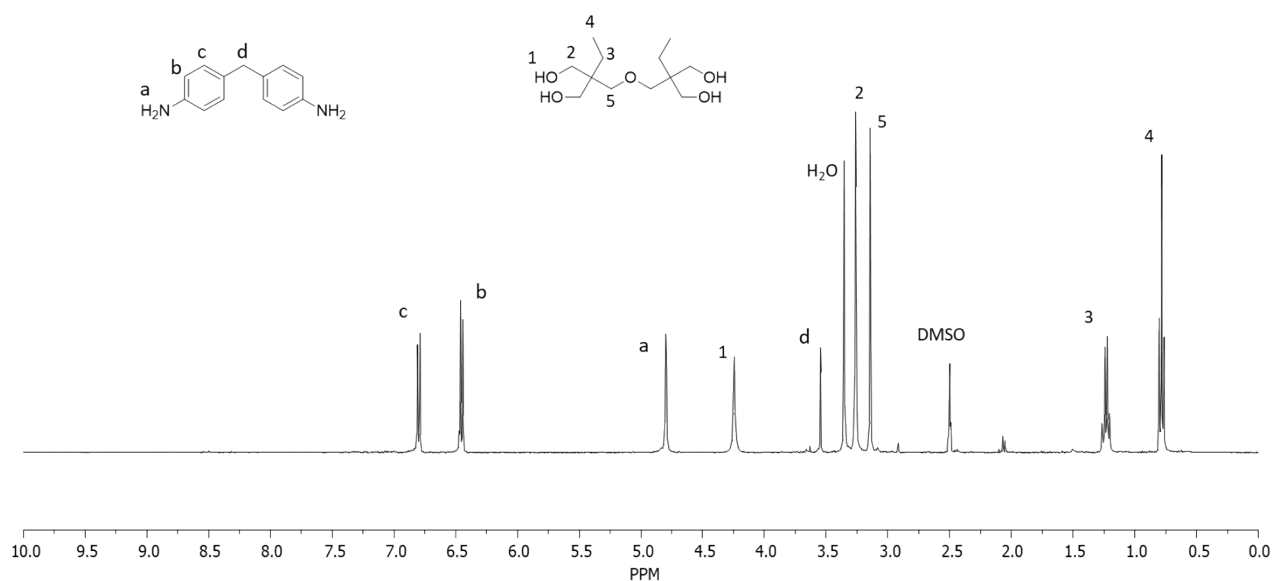


Figure S50. ¹H NMR spectrum in DMSO-d₆ of yielded material after hydrolysis of PAU-86 fibre for 52 days. The signals for di-TMP and 4,4-diaminodiphenylmethane were indicated.

Table S2. The yield of the recovered monomers.

Time	yield
24 h	69 % di-TMP 17 % MDA
48 h	77 % di-TMP 18 % MDA
52 days	73% di-TMP 22 % MDA

Table S3. Yield of the recovered monomers when using different solvents for extraction.

Solvent	diTMP	MDA
DCM	15 %	25 %
THF	84 %	20 %
ACN	64 %	20 %
MeOH	-	-

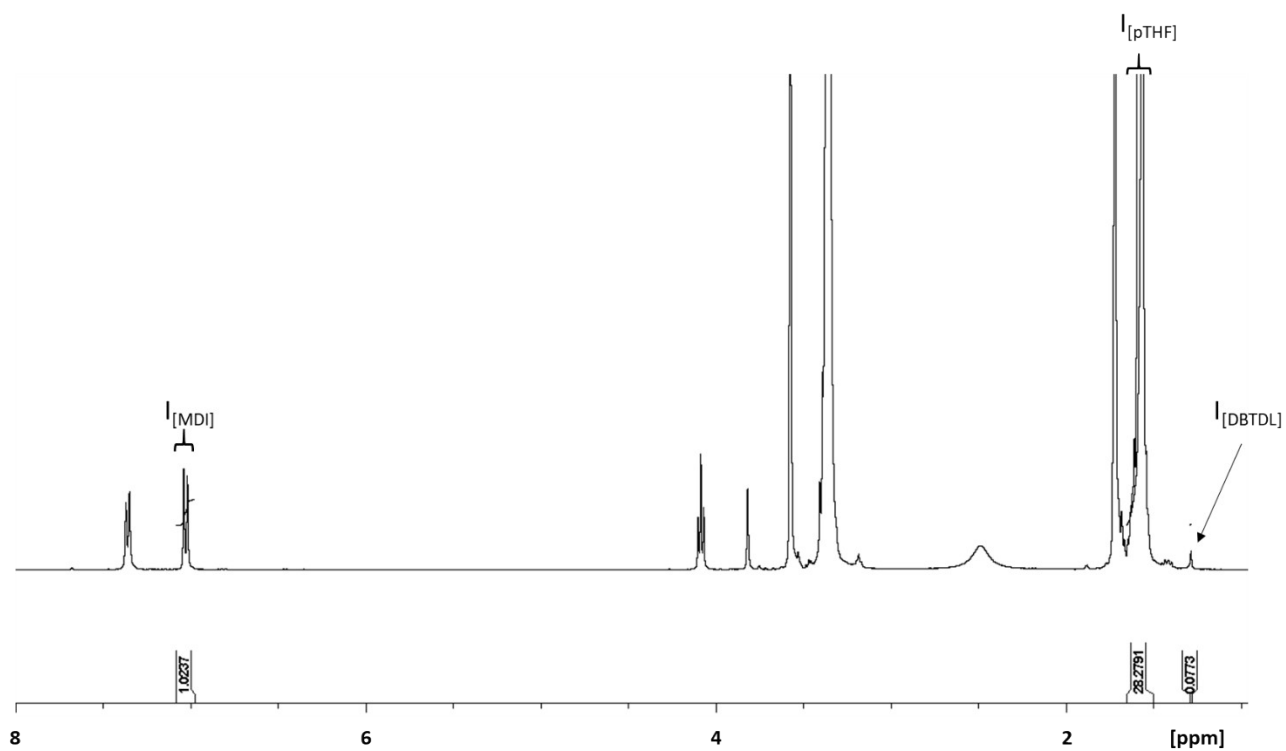


Figure S51. ^1H NMR spectrum of PAU-0. The signals necessary for calculating the DBTDL content were indicated. For assignments of all signals see Fig. 1.

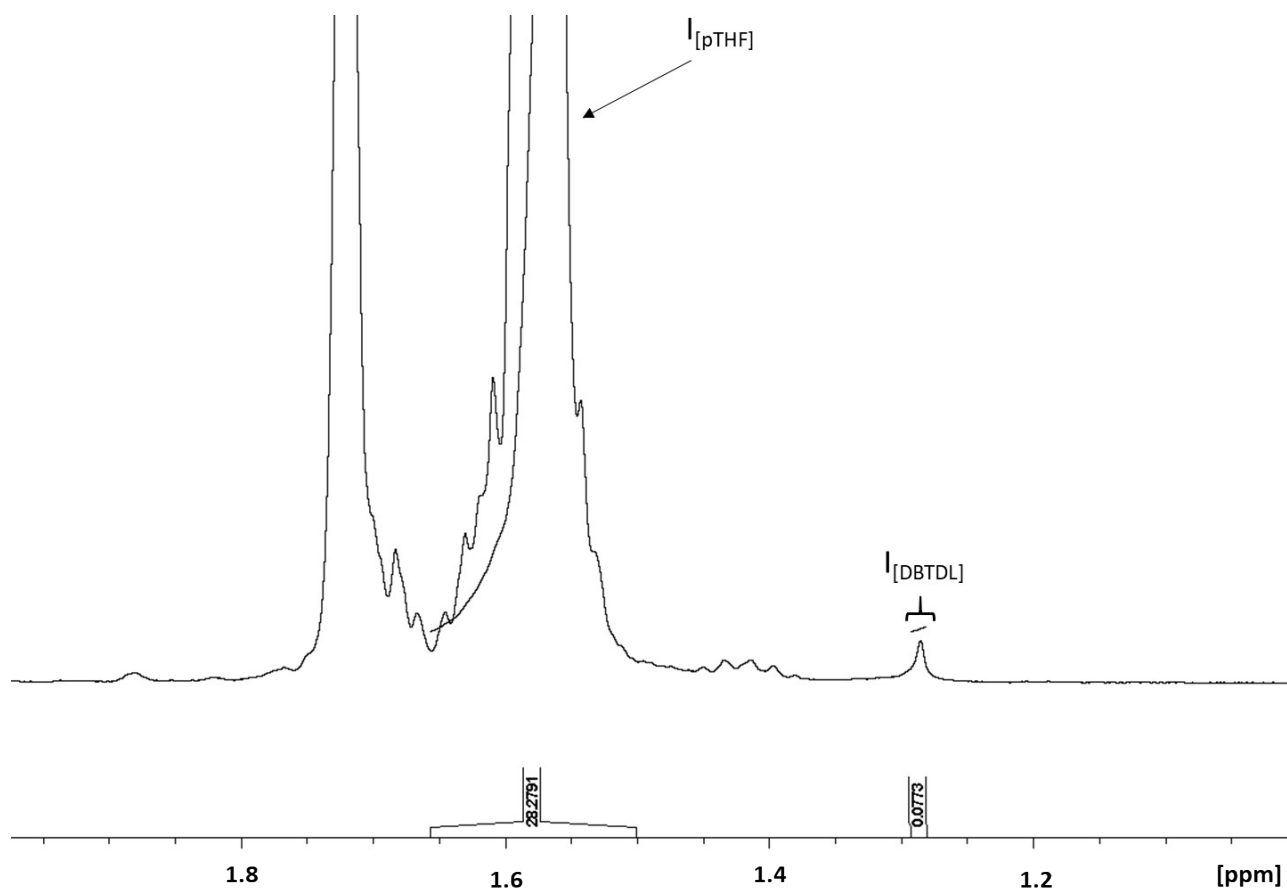


Figure S52. Zoomed-in ^1H NMR spectrum of PAU-0. The signals necessary for calculating the DBTDL content were indicated.

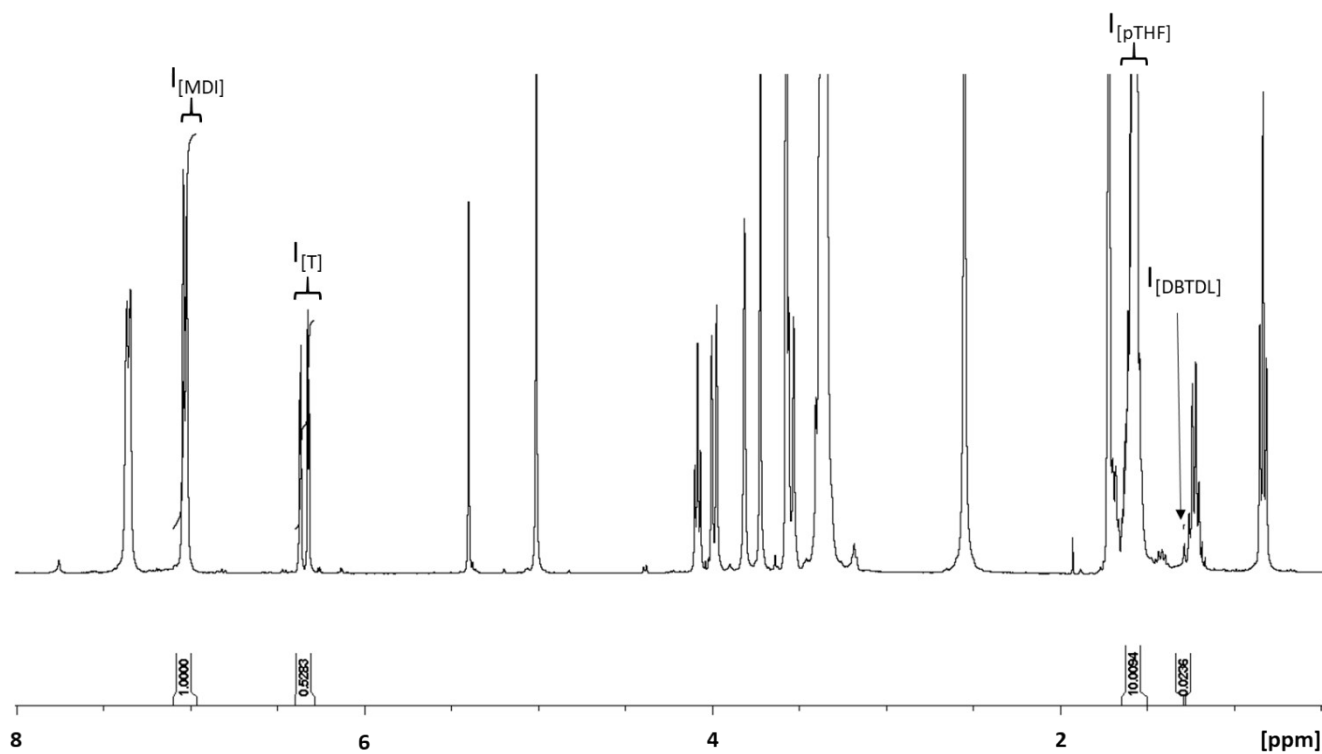


Figure S53. ^1H NMR spectrum of PAU-25. The signals necessary for calculating the DBTDL content were indicated. For assignments of all signals see Fig. 1.

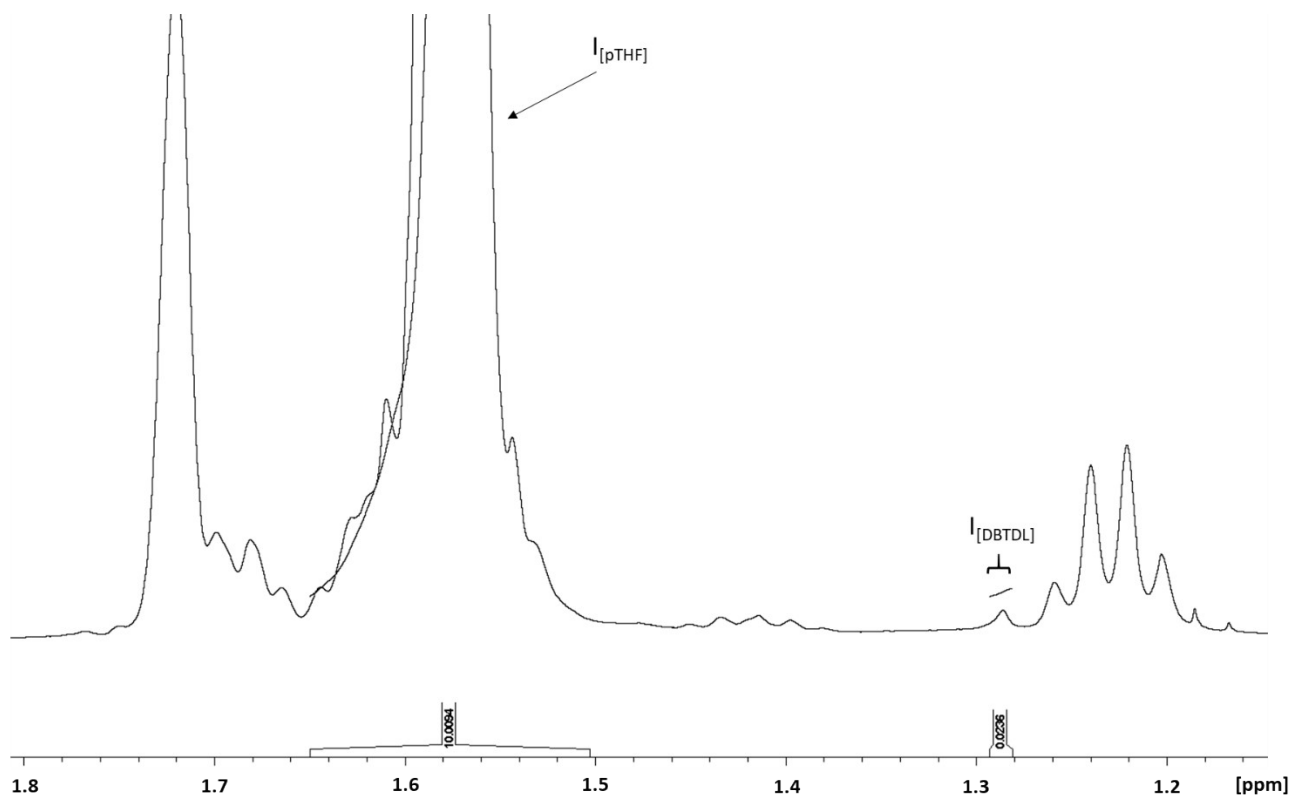


Figure S54. Zoomed-in ^1H NMR spectrum of PAU-25. The signals necessary for calculating the DBTDL content were indicated.

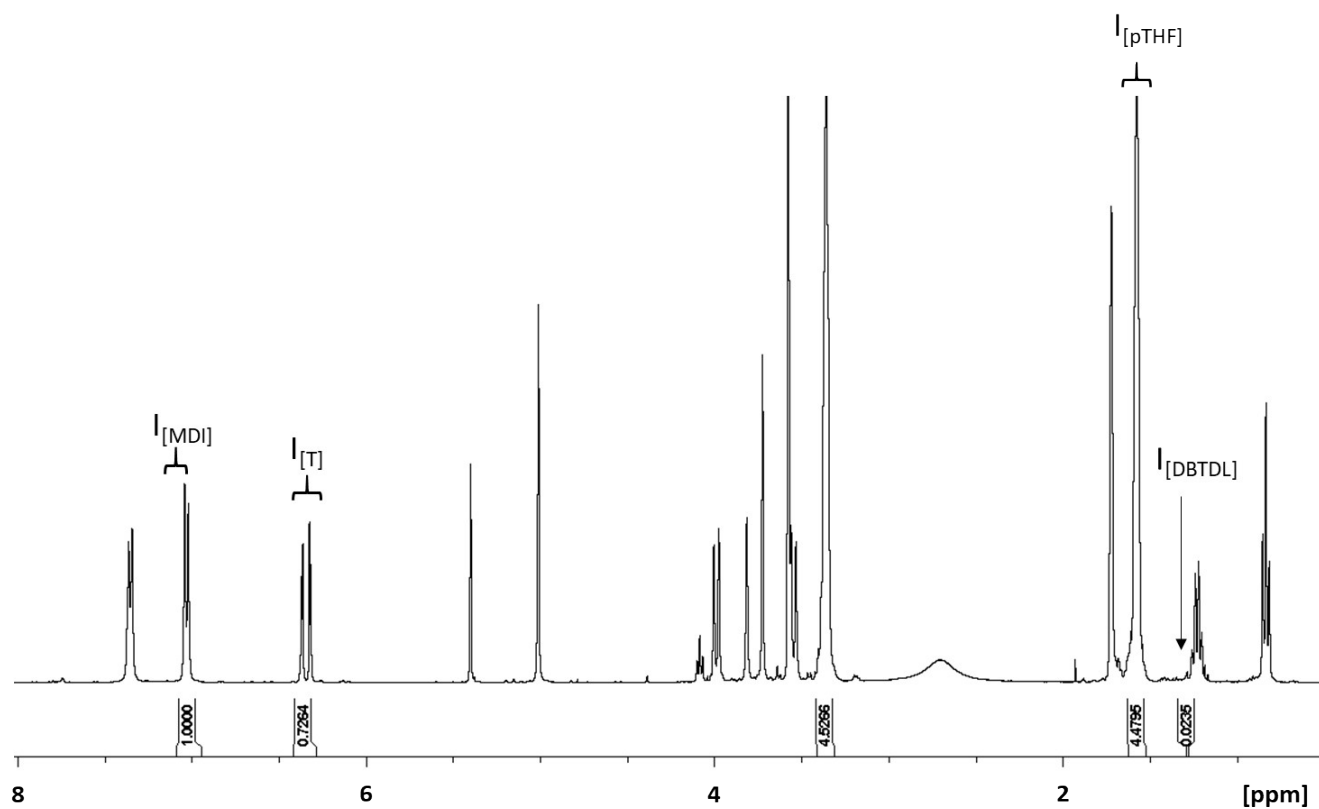


Figure S55. ^1H NMR spectrum of PAU-51. The signals necessary for calculating the DBTDL content were indicated. For assignments of all signals see Fig. 1.

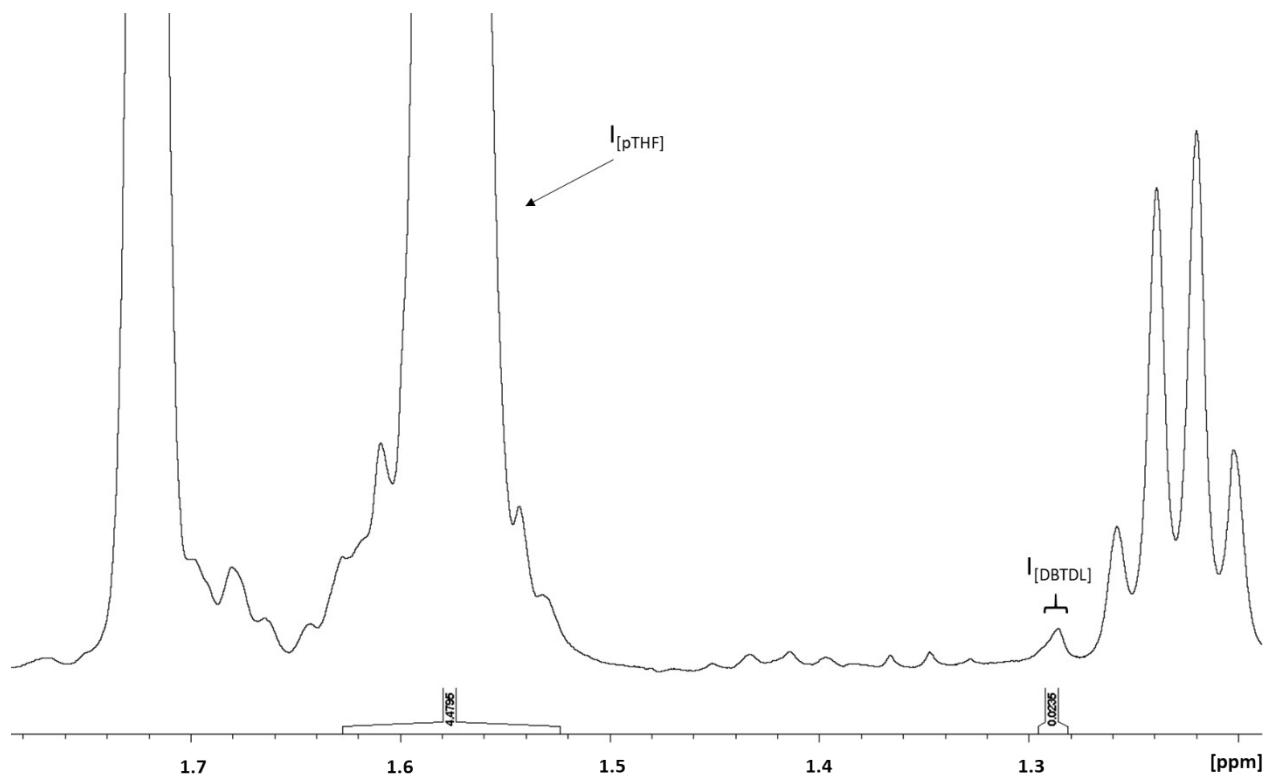


Figure S56. Zoomed-in ^1H NMR spectrum of PAU-51. The signals necessary for calculating the DBTDL content were indicated.

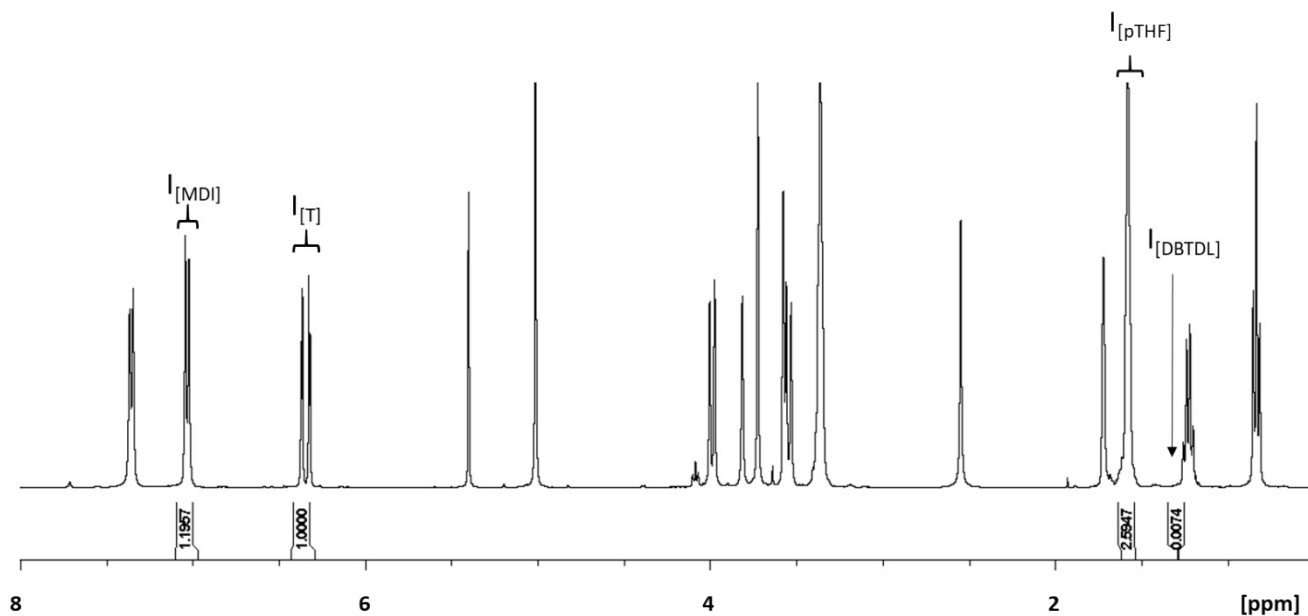


Figure S57. ^1H NMR spectrum of PAU-71. The signals necessary for calculating the DBTDL content were indicated. For assignments of all signals see Fig. 1.

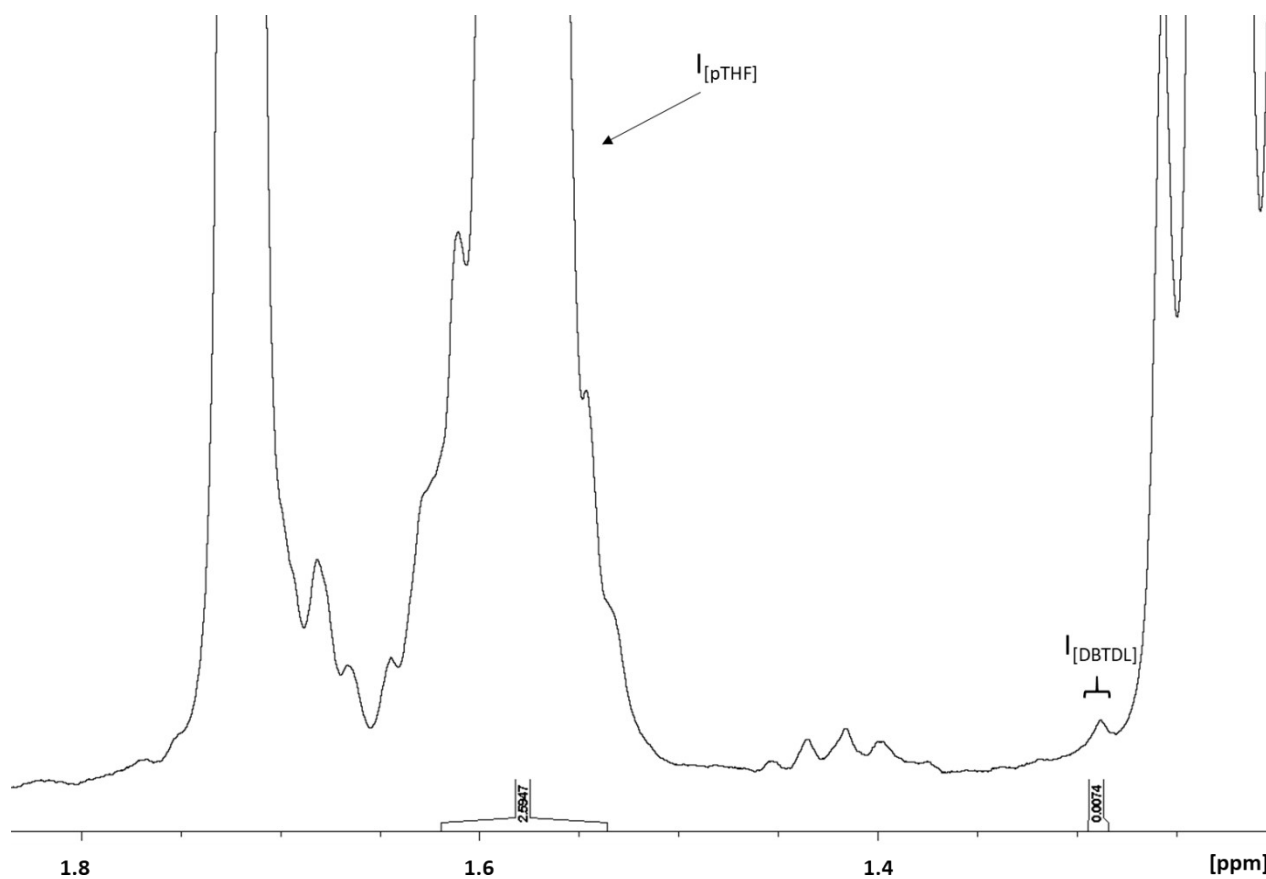


Figure S58. Zoomed-in ^1H NMR spectrum of PAU-71. The signals necessary for calculating the DBTDL content were indicated.

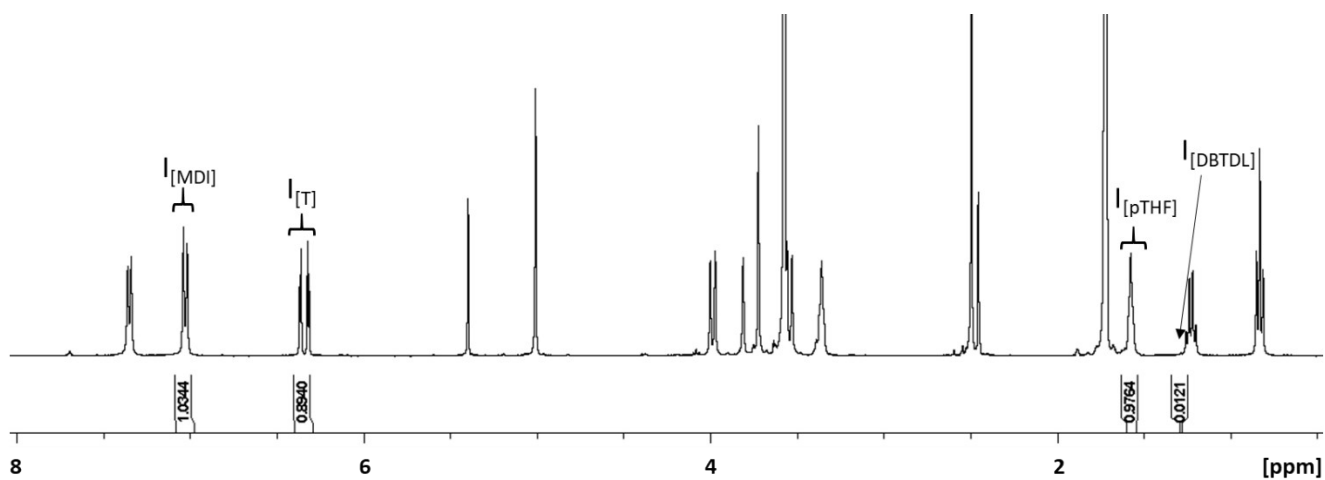


Figure S59. ^1H NMR spectrum of PAU-86. The signals necessary for calculating the DBTDL content were indicated. For assignments of all signals see Fig. 1.

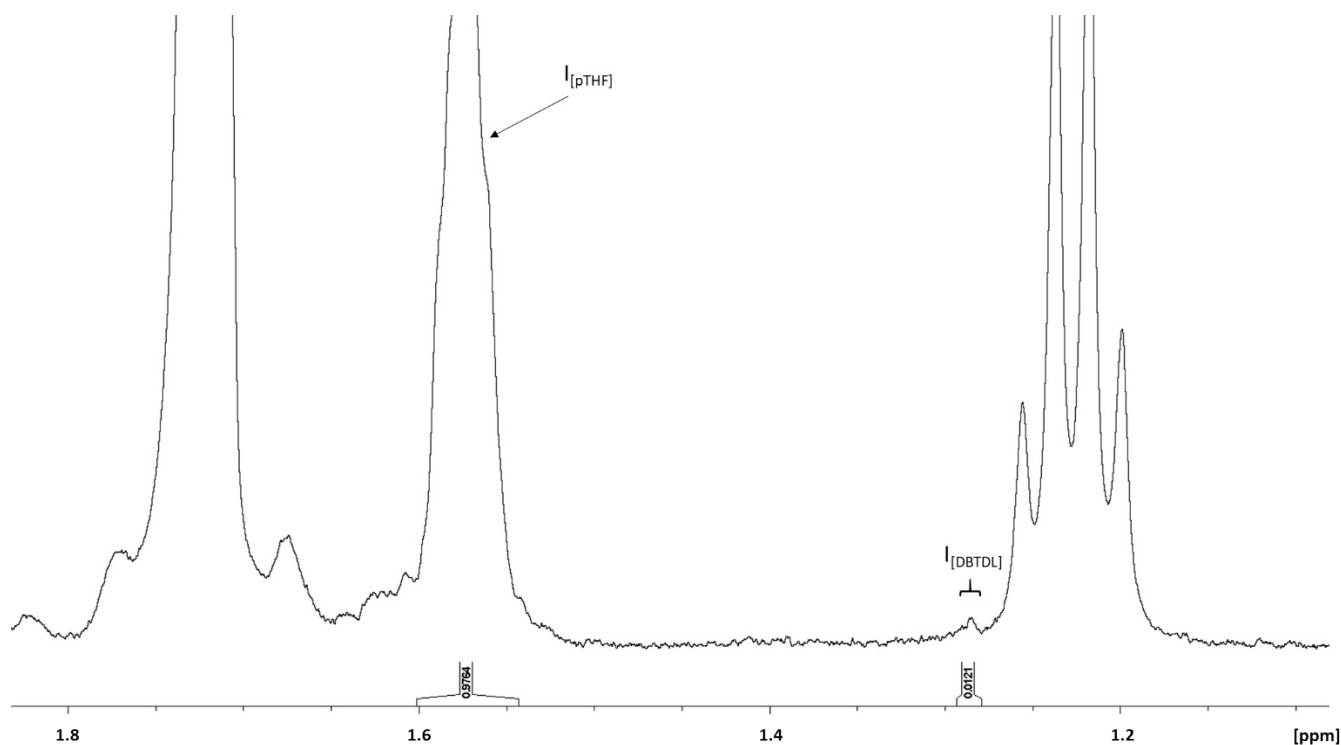


Figure S60. Zoomed-in ^1H NMR spectrum of PAU-86. The signals necessary for calculating the DBTDL content were indicated.

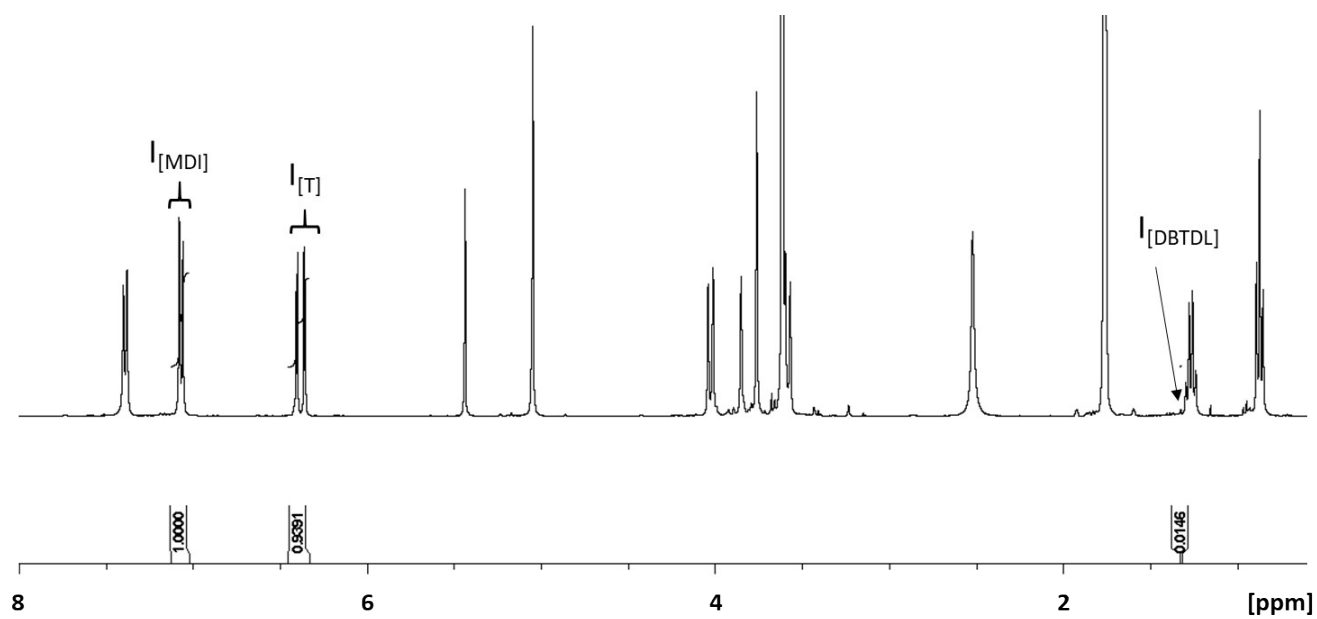


Figure S61. ^1H NMR spectrum of PAU-100. The signals necessary for calculating the DBTDL content were indicated. For assignments of all signals see Fig. 1.

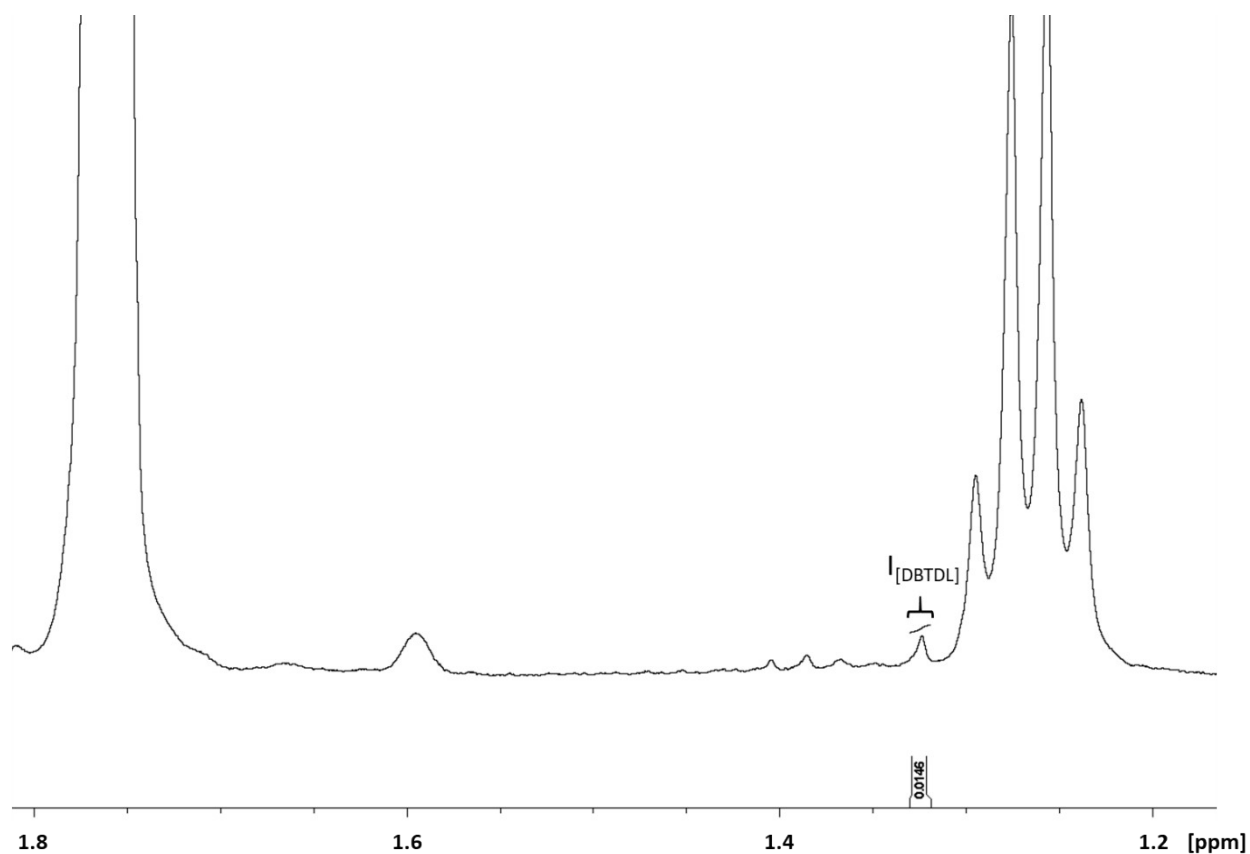


Figure S62. Zoomed-in ^1H NMR spectrum of PAU-100. The signals necessary for calculating the DBTDL content were indicated.

The catalyst content of the polymers was estimated using the method below:

$$M_{MDI} = 250.25 \text{ g/mol}$$

$$M_T = 466.52 \text{ g/mol}$$

$$M_{pTHF} = 2000.00 \text{ g/mol}$$

$$M_{DBTDL} = 631.56 \text{ g/mol}$$

The integrals used for each monomer were taken from Fig. S51-62. $I_{[MDI]}$ corresponds to 4 H on the MDI segment, $I_{[T]}$ corresponds to 4 H on the Monomer T segment, $I_{[pTHF]}$ corresponds to 111 H on the pTHF segment and $I_{[DBTDL]}$ corresponds to 44 H on the catalyst DBTDL.

The mass ratio (r_x) between the monomers was then estimated by dividing the integral with the corresponding number of protons (n_{H-x}), and then multiplied with the molecular mass of each monomer (M_x) individually:

$$\text{Eq. S1} \quad \frac{I_{[X]}}{n_{H-X}} * M_x = r_X$$

Where X represents the monomer or the catalyst.

Finally, the wt% DBTDL catalyst was calculated by dividing the mass ratio for DBTDL (r_{DBTDL}) with the total mass:

$$\text{Eq. S2} \quad \frac{r_{DBTDL}}{r_{MDI} + r_T + r_{pTHF} + r_{DBTDL}} * 100 = \text{wt\% DBTDL}$$

For example, the wt% DBTDL in PAU-86 was calculated below:

$$\frac{I_{[MDI]}}{n_{H-MDI}} * M_{MDI} = r_{MDI} = \frac{1.034}{4} * 250.25 = 64.69$$

$$\frac{I_{[T]}}{n_{H-T}} * M_T = r_T = \frac{0.894}{4} * 466.52 = 104.27$$

$$\frac{I_{[pTHF]}}{n_{H-pTHF}} * M_{pTHF} = r_{pTHF} = \frac{0.9764}{111} * 2000 = 17.59$$

$$\frac{I_{[DBTDL]}}{n_{H-DBTDL}} * M_{DBTDL} = r_{DBTDL} = \frac{0.0121}{44} * 631.56 = 0.1737$$

$$\frac{r_{DBTDL}}{r_{MDI} + r_T + r_{pTHF} + r_{DBTDL}} * 100 = \text{wt\% DBTDL}$$

$$\frac{0.1737}{64.69 + 104.27 + 17.59 + 0.1737} * 100 = 0.093 \text{ wt\% DBTDL}$$

Table S4. Catalyst content in the obtained polymers as estimated by the integrals of their corresponding ^1H NMR signals.

	wt % DBTDL
PAU-0	0.19
PAU-25	0.11
PAU-51	0.15
PAU-71	0.045
PAU-86	0.093
PAU-100	0.12